

# Lawrence Berkeley National Laboratory

## Recent Work

**Title**

ALPHA-DECAY STUDIES OF PROTACTINIUM ISOTOPES

**Permalink**

<https://escholarship.org/uc/item/5t35z26h>

**Author**

Subrahmanyam, Vishnu B.

**Publication Date**

1963-10-22

UCRL-11082

**University of California**  
**Ernest O. Lawrence**  
**Radiation Laboratory**

**TWO-WEEK LOAN COPY**

*This is a Library Circulating Copy  
which may be borrowed for two weeks.  
For a personal retention copy, call  
Tech. Info. Division, Ext. 5545*

**ALPHA-DECAY STUDIES  
OF PROTACTINIUM ISOTOPES**

**Berkeley, California**

## **DISCLAIMER**

This document was prepared as an account of work sponsored by the United States Government. While this document is believed to contain correct information, neither the United States Government nor any agency thereof, nor the Regents of the University of California, nor any of their employees, makes any warranty, express or implied, or assumes any legal responsibility for the accuracy, completeness, or usefulness of any information, apparatus, product, or process disclosed, or represents that its use would not infringe privately owned rights. Reference herein to any specific commercial product, process, or service by its trade name, trademark, manufacturer, or otherwise, does not necessarily constitute or imply its endorsement, recommendation, or favoring by the United States Government or any agency thereof, or the Regents of the University of California. The views and opinions of authors expressed herein do not necessarily state or reflect those of the United States Government or any agency thereof or the Regents of the University of California.

Research and Development

UCRL-11082

UC-4 Chemistry  
TID-4500 (24th Ed.)

UNIVERSITY OF CALIFORNIA  
Lawrence Radiation Laboratory  
Berkeley, California  
AEC Contract No. W-7405-eng-48

ALPHA-DECAY STUDIES OF PROTACTINIUM ISOTOPES

Vishnu B. Subrahmanyam  
(Ph. D. Thesis)

October 22, 1963

Printed in USA. Price \$1.75. Available from the  
Office of Technical Services  
U. S. Department of Commerce  
Washington 25, D.C.

# ALPHA-DECAY STUDIES OF PROTACTINIUM ISOTOPES

## Contents

Abstract . . . . .	v
I. Introduction . . . . .	1
II. Experimental Methods . . . . .	2
A. Alpha Spectroscopy	
1. Surface Barrier Detectors . . . . .	2
2. Double-Focusing Alpha-Particle Spectrograph . . . . .	2
B. Alpha-Particle Gamma-Ray Coincidences . . . . .	3
C. Preparation and Purification of Samples. . . . .	9
III. Observations	
A. Alpha Decay of Pa <sup>227</sup> . . . . .	12
1. Alpha Spectrum . . . . .	12
2. Gamma Spectrum . . . . .	12
3. Decay Scheme . . . . .	15
4. Interpretation of Levels. . . . .	20
B. Alpha Decay of Pa <sup>229</sup> . . . . .	30
1. Ground State . . . . .	30
2. Gamma Rays . . . . .	32
3. Decay Scheme and Spin Assignments . . . . .	43
4. Interpretation of Levels. . . . .	49
C. Alpha Decay of Ac <sup>223</sup> . . . . .	49
1. Alpha Spectrum . . . . .	50
2. Gamma Rays . . . . .	54
3. Decay Scheme and Interpretation of Levels . . . . .	57
D. Other Experiments. . . . .	60
1. Alpha Spectrum of Pa <sup>231</sup> . . . . .	60
2. Gamma-Gamma Coincidences. . . . .	62
Acknowledgments. . . . .	65
References . . . . .	66

## ALPHA-DECAY STUDIES OF PROTACTINIUM ISOTOPES

Vishnu B. Subrahmanyam

Lawrence Radiation Laboratory and Department of Chemistry  
University of California, Berkeley, California

October 22, 1963

### ABSTRACT

The alpha decay of  $\text{Pa}^{231}$ ,  $\text{Pa}^{229}$ ,  $\text{Pa}^{227}$ , and  $\text{Ac}^{223}$  is studied. An alpha-particle — gamma-ray coincidence technique was employed. We used a 180 deg double-focusing spectrograph or gold-silicon solid-state detectors for alpha analysis, and a sodium iodide (Tl-activated) scintillation crystals for gamma-ray detection.

The ground states of  $\text{Pa}^{227}$  and  $\text{Pa}^{229}$  are shown to be populated by 5.46- and 5.73-MeV  $\alpha$  particles, respectively. The rotational bands populated in the decay of  $\text{Pa}^{227}$  are interpreted as being based on octupole vibrational levels predicted by the Bohr-Mottelson "strong-coupling" model. Modified decay schemes are presented.

It is suggested that in odd-proton nuclei, the permanent nuclear deformation starts closer to the closed shell than in the even-even nuclei.

A new alpha group at 5.47 MeV is reported in the alpha decay of  $\text{Ac}^{223}$ . No rotational structure is observed in the levels populated.

Evidence is presented for the presence of two additional levels populated in the alpha decay of  $\text{Pa}^{231}$ .

## I. INTRODUCTION

A number of theoretical models have been proposed to explain the properties of the nucleus. Experimental techniques, which are being constantly improved, have helped us test these theories and understand the nuclear-decay processes. The shell model of the nucleus originally proposed by Mayer<sup>1</sup> and Jensen<sup>2</sup> describes the properties of spherical nuclei, while the strong-coupling "collective model" by Bohr and Mottelson<sup>16</sup> successfully explains the nuclear properties of heavy elements having nuclei known to possess a non-spherical but axially symmetric equilibrium shape.

In the periodic table where both the proton and neutron shells are filled (in the isotope  $\text{Pb}^{208}$ ), the equilibrium shape of the nucleus is known to be spherical. In the heavier elements ( $A > 225$ ), an existing permanent spheroidal deformation explains the rotational nature of the observed levels. In the intermediate region the level structure is not very well understood. Also, experimenters have observed that the level structure becomes more complex for the odd-mass nuclei. A study of the alpha decay of  $\text{Pa}^{229}$  and  $\text{Pa}^{227}$  is undertaken to gather information that may help extend the present theories of nuclear structure to elements of the intermediate region of deformation. The alpha decay of  $\text{Ac}^{223}$  is also studied.



## II. EXPERIMENTAL METHODS

Two types of nuclear spectroscopy--alpha and gamma--have been employed here. The alpha spectra were obtained with either a double-focusing electromagnetic spectrograph or with surface-barrier solid-state detectors. Thallium-activated sodium iodide crystals were used to detect the  $\gamma$  rays. The  $\gamma$ -ray spectra were obtained through  $\alpha$ -particle— $\gamma$ -ray coincidence measurements. Details of these experiments and the preparation and purification of samples are presented in the following section.

### A. Alpha Spectroscopy

#### 1. Surface Barrier Detectors

These detectors may be considered to be solid-state ionization chambers; they consist of thin wafers of silicon crystals coated with gold on one side. A positive voltage bias was applied across the crystal and the  $\alpha$  particles striking the gold surface created an electric impulse when stopped in the depletion layer. This signal, proportional to the  $\alpha$ -particle energy, was then amplified and pulse-height-analyzed. Different sizes of detectors were used, depending on the resolution and geometry considerations. Full details of construction and maintenance of these detectors are available in the literature.<sup>34</sup>

#### 2. Double-Focusing $\alpha$ -Particle Spectrograph

This instrument is a modified Siegbahn-Svartholm double-focusing spectrograph. The magnetic field is nonuniform, with a radial dependence that produces focusing in both vertical and horizontal directions. The field is shaped to permit the location of both sample and receiver outside the magnetic field. The magnet covers 180 deg with a maximum radius of 50 cm and an optical axis of 35-cm radius. The field along the normal axis is proportional to the measured frequency of a  $\text{Li}^7$  nuclear-magnetic resonance probe located at 9-cm radius. The receiver was either a photographic plate or an array of solid-state detectors 1.5 mm wide and 10 mm long.

The path of the  $\alpha$  particles reaching the receiver can be restricted by adjustable baffles at 90 deg radius. The photographic plates used to record the spectra were scanned every 1/4 mm along the width under a microscope. The total number of tracks at each position was plotted against the position, this position being proportional to the energy of the  $\alpha$  particle. The energies of the various peaks observed with Pa<sup>227</sup> sources were calculated relative to the two peaks of Bi<sup>211</sup>, whose energies were known accurately.<sup>5</sup> The dispersion and the peak shape depended on the position of occurrence on the plate. The change in peak shape was shown to be caused by the focusing at different positions on the receiver of  $\alpha$  particles of single energy traveling in paths farther away from the optical axis. We corrected this constructional defect of the magnet by changing the pole shape of the magnet on the source side, thereby achieving improved transmission of the  $\alpha$  particles. The exact shape of the pole face was determined by observing the focusing of single-energy  $\alpha$  particles traveling away from the normal axis. Through this modification all  $\alpha$  particles of the same energy crossing the 90-deg radius between 25 cm and 44 cm could be brought to focus at the same position.

#### B. Alpha-Particle — Gamma-Ray Coincidences

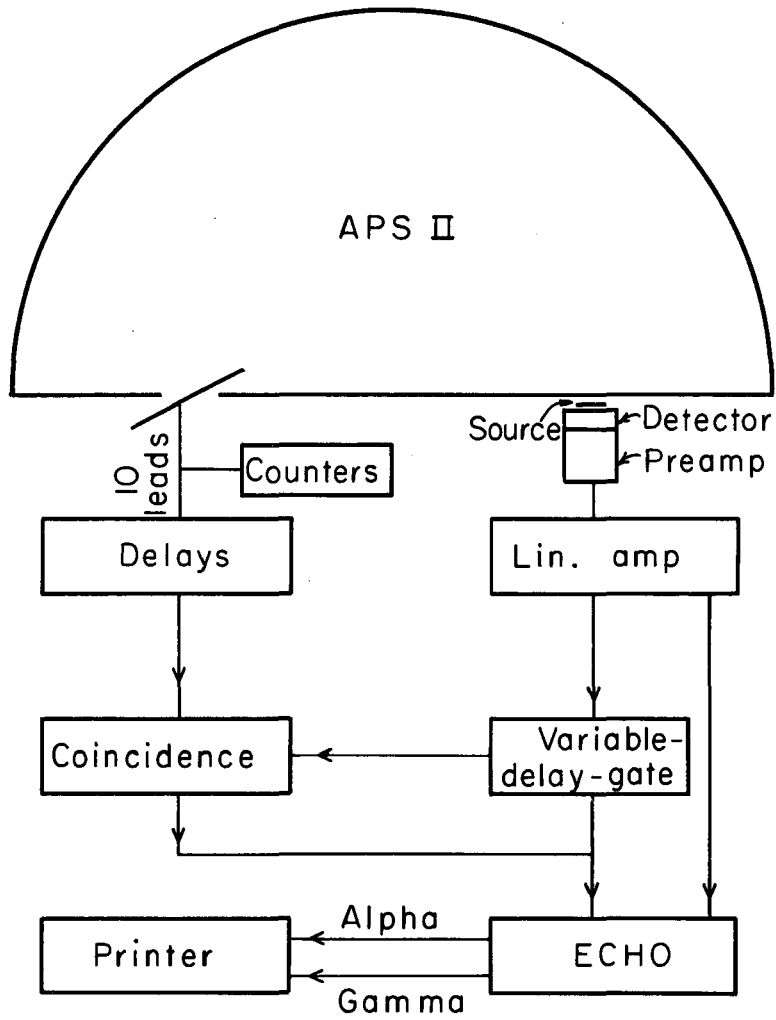
The  $\gamma$  rays arising from the internal transitions could be detected only through coincidence techniques because of the high levels of extraneous gamma activity associated with the prepared samples. Further, the closely spaced levels demanded an alpha detector of high resolution. For this purpose the double-focusing spectrograph was employed in which an array of ten solid-state detectors was used as the receiver. The magnetic field was so adjusted as to focus an alpha group among two or three detectors. The whole array accommodated about 60-keV energy range.

The  $\gamma$  rays were detected by a NaI (Tl-activated) crystal mounted on a phototube (DuMont 6292). The light output of the detector was converted into an electric pulse by the phototube, then amplified and used on the gamma side of the coincidence setup. Two sizes

of crystals were used, one of 3 in. diam and 3 in. long, the other of 1.5 in. diam and 1.5 in. long. The latter was provided with a beryllium window and was more useful in the investigations of the L x-ray region.

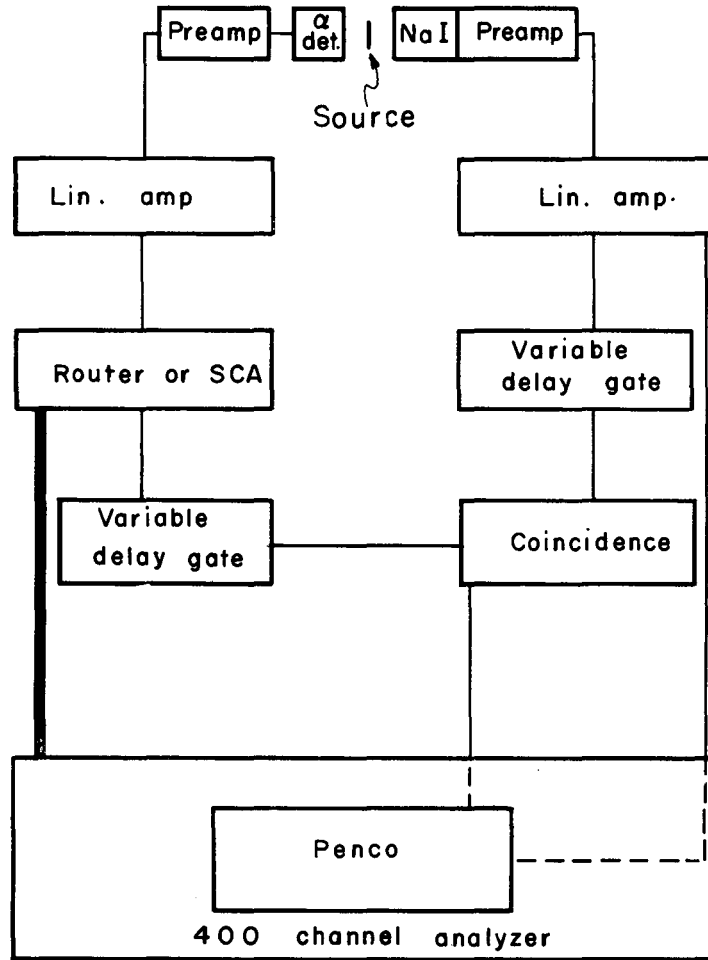
The arrangement for the coincidence measurements when the magnetic alpha spectrometer is employed is represented schematically in Fig. 1. The details of its working were described by others<sup>6</sup> and therefore are here mentioned only briefly. The electrical pulses from each one of the detectors in the array on the alpha side were amplified, counted, and fed into a coincidence unit that puts out a "coincidence pulse" when a gate generated by the gamma pulses is also present at the same time. The coincidence pulse acts as a gate for an ECHO analyzer where the coincident  $\gamma$  ray was pulse-height-analyzed. The ECHO analyzer also operated a printer that records the number identifying the alpha detector and the  $\gamma$ -ray energy. The  $\gamma$ -ray spectrum in coincidence with a given alpha group was then compiled from these data. The corrections for accidental coincidences were determined separately by replacing the alpha pulses by artificial electronic pulses; these corrections were subtracted from the observed data. The background counts for each detector on the alpha side were determined and subtracted from the number of counts recorded during the experiment and the intensities of the coincident  $\gamma$  rays were calculated. The whole experimental arrangement was aligned and calibrated using the 60-keV  $\gamma$  ray in the alpha decay of  $\text{Am}^{241}$ .

In the decay of  $\text{Ac}^{223}$  the  $\alpha$  particles were detected by surface-barrier detectors and the experimental arrangement for coincidence measurements is represented in Fig. 2. The amplified alpha pulses were fed into a router that consisted of four single-channel pulse-height analyzers that operated one at a time. The analyzers were adjusted to pass pulses corresponding to the  $\alpha$  particles of  $\text{Ac}^{223}$ . The outputs were counted individually to determine the intensity of the coincident  $\gamma$  rays. The output of the router operated a variable delay gate and the corresponding quadrant of a 400-channel pulse-height analyzer. The  $\gamma$  rays detected by a NaI crystal were amplified and fed to the 400-channel analyzer and to a variable delay gate. The



MU-30095

Fig. 1. Block diagram for coincidence measurements using APS II.

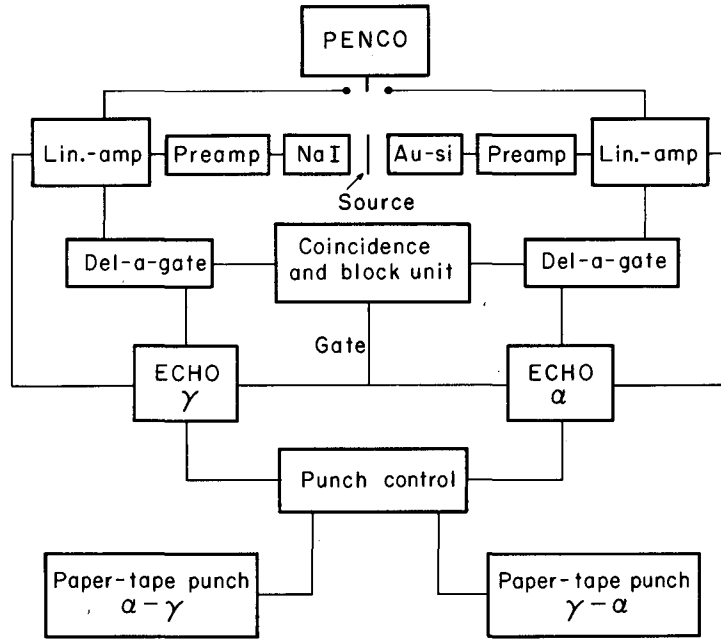


MU-30099

Fig. 2. Schematic of alpha-gamma coincidence measurements.

shaped pulses from the delay-gates, properly delayed, were placed in coincidence with a resolving time of 1  $\mu$ sec. The pulse from the coincidence unit opened the gate of the pulse-height analyzer, which analyzed the coincident  $\gamma$  ray and stored it in the appropriate quadrant. This arrangement allowed us to study all the alpha groups simultaneously. When  $\gamma$  rays in coincidence with only one alpha group were measured, the router was replaced by a single-channel analyzer in combination with a 100-channel pulse-height analyzer.

The  $\alpha$ -particle— $\gamma$ -ray coincidence arrangement used for Pa<sup>229</sup> sources is represented in Fig. 3. A two-dimensional analysis and coincidence technique was employed in place of a single-channel pulse-height analyzer for energy discrimination of the  $\alpha$  particles. The arrangement, as represented, is a combination of the punch-tape unit<sup>7</sup> and the coincidence unit.<sup>6</sup> The  $\alpha$  and  $\gamma$  pulses from the respective linear amplifiers were fed into two separate ECHO analyzers operated by a coincidence gate. The coincidence gate was formed when the shaped pulses from the variable delay-gates on both sides arrived at the same time. The resolving time used was 0.5  $\mu$ sec and was determined by the width of the two pulses. After the formation of the gate that opened the analyzers that analyzed the respective pulses, and after the pulse-height information was fed to the punch-tape control, the coincidence unit was made inoperative. The coincidence data were recorded in two ways on two different tapes; the alpha or the gamma pulse-height information appeared first. This facilitated the decodification of the data. The gross alpha spectrum was also recorded separately on a 100-channel Penco pulse-height analyzer during the experiment. The gamma spectrum in coincidence with an alpha group was obtained from the tapes with the help of a punch-tape reader. The information which appeared first on the tape was analyzed by a single-channel analyzer (SCA) of the reader and if the data were to fall within the two preset boundaries of the SCA, the following information was analyzed and stored. Similarly, using the tapes with the gamma information appearing first, it was also possible to obtain the alpha spectrum in coincidence with any given region



MU-32884

Fig. 3. Block diagram of two-dimensional analysis coincidence measurements.

of the gamma spectrum. The arrangement was calibrated by using a standard Am<sup>241</sup> sample.

### C. Preparation and Purification of Samples

The protactinium-227 used in these studies was prepared by bombardment on the end of thorium-232 foils with deuterons of minimum available energy, 150 MeV. Thorium foils 0.010 in. thick and measuring  $0.75 \times 0.5$  in. were wrapped in 0.001-in. platinum foil and introduced into the 184-in. synchrocyclotron. At the minimum approachable radius, a deuteron beam of 0.5  $\mu$ A was obtained. Under these conditions, various isotopes of protactinium were formed almost in equal amounts. The half lives and the modes of decay of these isotopes are indicated in Table I. Following 1-hr bombardments, thorium foils were dissolved in about 15 ml of hot conc HCl to which dilute HF was added drop by drop. On some occasions, a white precipitate (believed to be thoria) was observed; this was removed. The excess flouride in the solution was eliminated by adding a saturated borate solution. The clear solution was then transferred onto a 5-mm diam column packed with 2.5 to 3.0 cm of Dowex 1A (400  $\mu$ , 8% cross linkage) anion-exchange resin. The column was pressurized to increase the flow rate but not to exceed 2 drops per second. Thorium passed through without adsorption while the other actinides remained on the column. The resin was washed successively with 3 to 4 times its volume of conc HCl, 10 M HCl, and 6 M HCl. Protactinium isotopes were eluted with 1 ml of 9 M HCl containing 0.1 M HF and evaporated to dryness. The activity, consisting mainly of protactinium isotopes and some uranium, was transferred to another box where it was further purified by adsorption on an anion-exchange resin column 2 mm in diam, and 1 cm long. The cleanup column was first washed with 10 M and 6 M HCl and protactinium was eluted from this cleanup column by 5 to 6 drops of 2.7 M HCl, and evaporated on a platinum disc. The line sources were prepared by vacuum sublimation of the activity onto 0.002-in. aluminum discs. Alpha activities actually used in the experiments were restricted to  $2 \times 10^6$



Table I. Protactinium isotopes formed  
in the bombardments.

Isotope	Half life	Mode of decay		No. of states populated	
		alpha (%)	EC (%)	alpha	EC
Pa <sup>230</sup>	17 day	--	--	--	--
Pa <sup>229</sup>	1.5 day	0.25	99	13	2
Pa <sup>228</sup>	22 hr	2	98	27	13
Pa <sup>227</sup>	38.3 min	85	15	9	--

disintegrations per minute so as to minimize chance coincidences resulting from the high gamma activity from the other isotopes of protactinium. The total time required for the chemical separation and sample preparation was about 1 hr.

Protactinium-229 was obtained as the electron-capture decay product of uranium-229. Uranium-229 was prepared by bombarding thorium-232 foils of 1 in. on end with the minimum available energy  $\alpha$  particles of 280 MeV. Following 1-hr bombardments, the foils were dissolved in conc HCl (with some HF) and adsorbed on an anion-exchange resin. All the actinide elements except uranium were washed off with HCl of various concentrations, and 9 M HCl plus 0.1 M HF was used to remove any directly formed protactinium. Protactinium-229 was eluted with 2.7 M HCl after the complete decay of uranium-229 and further purified in a cleanup column. This method provided isotopically pure Pa<sup>229</sup>, but the amounts were not enough for the experiments. The required amount of activities were prepared by bombarding Th<sup>232</sup> with protons of 25-MeV energy from the 88 inch cyclotron. Protactinium was separated chemically from the targets following 4- to 5-hr bombardments amounting to 15 to 20  $\mu$ A.hr.

Actinium-223 samples were obtained by repeated 3-min collections of the recoils from the parent. Protactinium-227 was sublimed as a thin layer onto a metallic disc and the recoiling atoms were collected on another disc 1 in. away in the atmosphere. A potential difference of 1500 V was maintained between the source (positive) and the collector (negative). Better collection efficiency was achieved by making the sources thinner and by collecting the recoils at the center of a cylinder with the source vaporized onto the inside surface of the cylinder. Three-minute collections appeared to contain the optimum amounts of actinium. Attempts to remove the directly collected bismuth by flaming the collection plates did not prove profitable.

### III. OBSERVATIONS

#### A. Alpha Decay of Pa<sup>227</sup>

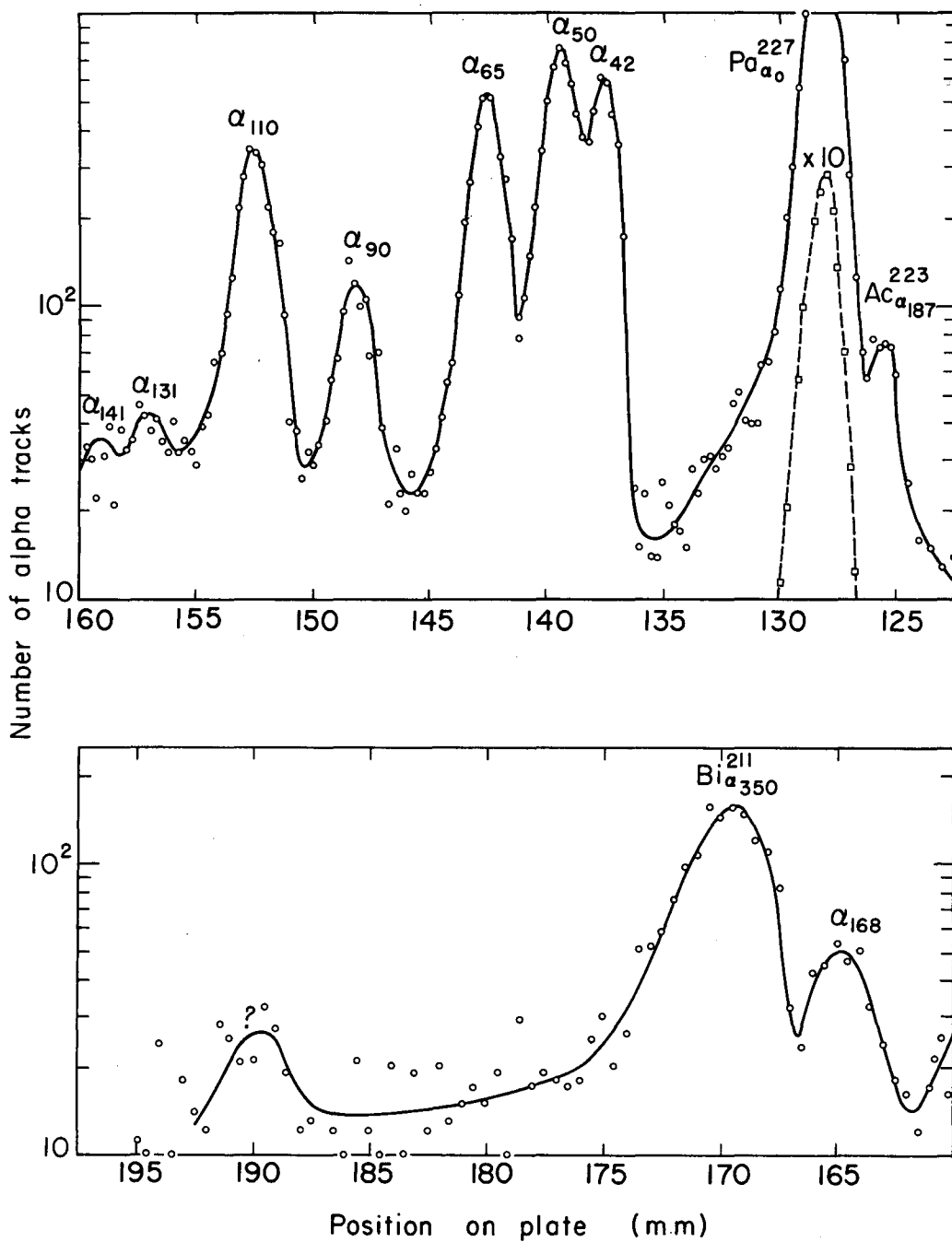
Protactinium-227 was first prepared by Meinke,<sup>8</sup> who determined its half life to be 38.3 min with an alpha decay branching of 85%. The energy of the  $\alpha$  particle associated with its decay was determined to be 6.46 MeV. The fine structure of the alpha spectrum was studied by Hill,<sup>9</sup> who proposed that the 6.46 MeV alpha group led to an excited state at 67.3 keV; he also suggested the presence of a rotational band ( $K = 5/2$ ) based on this level. This suggestion was based purely on the observed energy spacings and intensities of the various levels. A systematic study of  $\alpha$ -particle— $\gamma$ -ray coincidences was undertaken to establish a decay scheme.

##### 1. Alpha Spectrum

The various groups identified in the alpha spectrum represented in Fig. 4 are based on the present studies. The spectrum is quite similar to that obtained by Hill with the important difference that groups of higher energy than 6.46 MeV are interpreted as not belonging to the Pa<sup>227</sup> decay. The energies of the various levels shown in Table II come from alpha groups determined relative to the two alpha groups of Bi<sup>211</sup> (which was present in equilibrium with Pa<sup>227</sup>) and whose energies were determined accurately by Pilger.<sup>5</sup>

##### 2. Gamma Spectrum

The method of preparation of sources makes it impossible to obtain pure Pa<sup>227</sup> free from other alpha emitters. Owing to the presence of other isotopes of protactinium the samples also exhibited high levels of gamma activity. Coincidence techniques (described in Sec. II) were employed to observe the  $\gamma$  rays; we used the double-focusing spectrograph for detecting selectively the closely spaced alpha groups.



MUR-1743

Fig. 4. Alpha spectrum of  $\text{Pa}^{227}$ .

Table II. Alpha groups of Pa<sup>227</sup>.

Alpha-particle energy (MeV)	Excited-state energy (keV)	Abundance (%)		Hindrance factor <sup>a</sup>
		Hill's work	This work	
6.460	0.0	49.5	50.7	2.6
6.418	42.4	11.5	11.8	7.4
6.410	50.8	14.8	15.2	5.3
6.396	64.7	9.3	9.6	7.3
6.371	90.6	2.6	2.6	20
6.351	110.3	7.8	8.0	5.6
6.331	131.3	0.7	0.7	50
6.321	141.3	0.4	0.4	80
6.294	168.3	0.8	0.8	30

a. Hindrance factor values taken from reference 37.

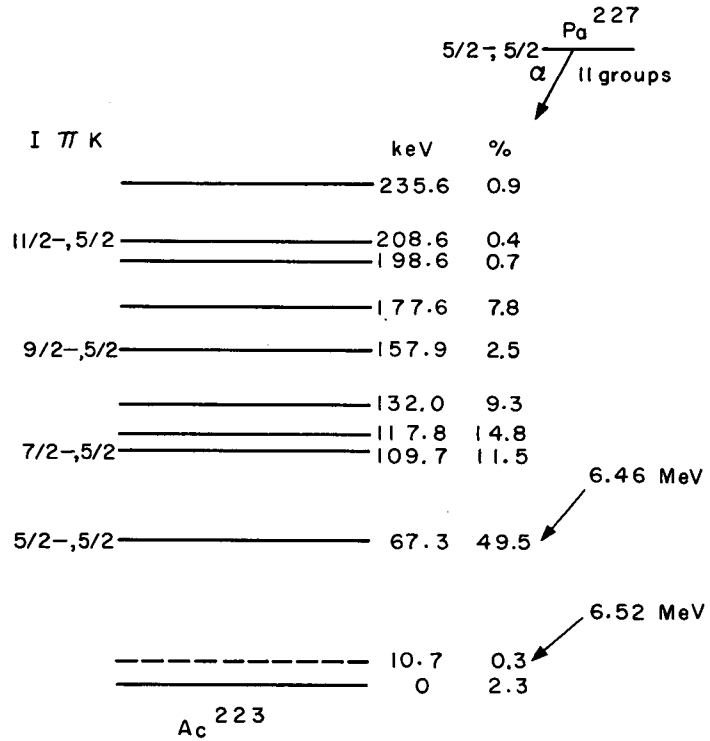
### 3. Decay Scheme

The decay scheme proposed by Hill (see Fig. 5) represents the ground state as being populated by 6.52-MeV alpha particles. On this basis, the intense 6.46-MeV group is expected to be in coincidence with photons or conversion electrons or both. Neither  $\gamma$  rays nor conversion x rays were observed in coincidence. On the assumption that an isomeric state is involved, delayed-coincidence experiments were conducted. In the investigated range of 1  $\mu$ sec to 0.5 min half life, the observed coincidences were enough to account for the expected chance coincidences. These negative results led to the present assignment in Fig. 8. (see alpha decay of  $\text{Ac}^{223}$ ). The results of the coincidence measurements are presented below, where the separate levels are discussed.

a. 42-keV level. No  $\gamma$  rays of measurable intensity were observed in coincidence with the  $\alpha$ 's populating this level, and the intensity of the observed L x rays accounted for the intensity of the group, which suggested an E2 transition consistent with the assignment of this level as a member of the ground-state rotational band.

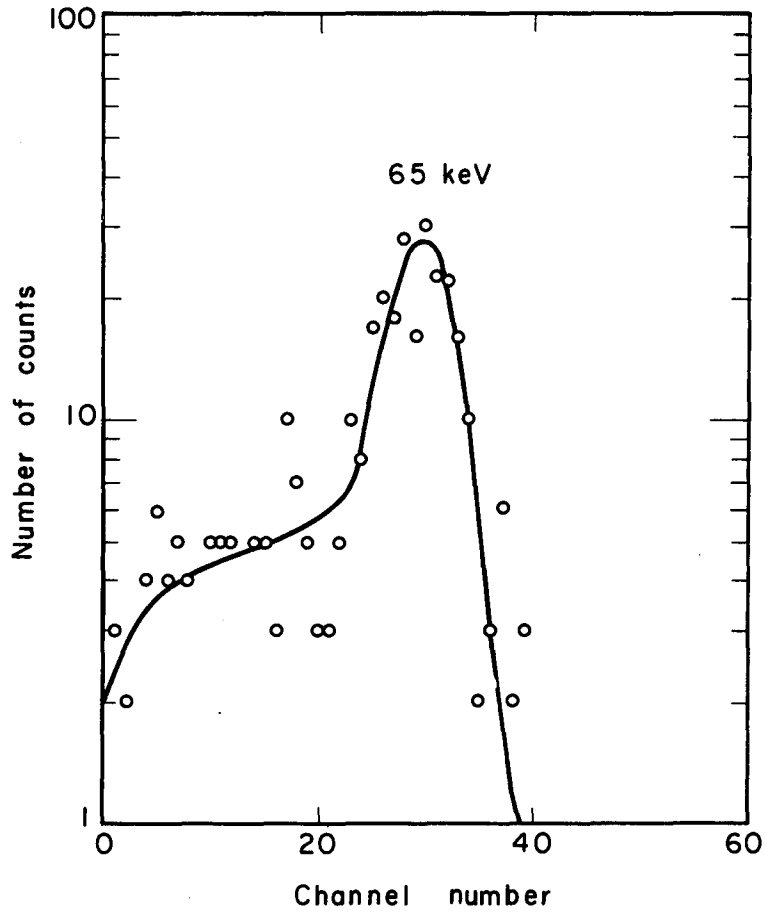
b. 50-keV state. Both L x rays and a  $\gamma$  ray of approximately 50 keV were observed in coincidence with  $\alpha$  particles leading to this state. The intensity of the photon could not be determined with certainty because of the strong E1 transition from the next highest level and because of the inherent limitations on the alpha resolution. This means that there is not a 50-keV E1 transition in coincidence with this alpha group. However, an upper limit of 0.02 photon per  $\alpha$  decay can be set on the intensity of this  $\gamma$  ray, which gives a minimum value for the conversion coefficient of 6.5. The theoretical conversion coefficients for E1, E2, M1, and M2 are 0.7, 275, 22.7, and 1050, respectively. This allows a reasonable choice of M1 or E2 or a mixture of both for this transition.

c. 65-keV level. The gamma spectrum observed in coincidence with the  $\alpha$  particles populating this state is presented in Fig. 6. The intensity of the 65-keV  $\gamma$  ray was found to be 6.2% of the total alpha decay, while this level is populated to the extent of 9.6%, which gives



MU-30097

Fig. 5. Decay scheme of  $\text{Pa}^{227}$  (by Hill).



MU-30096

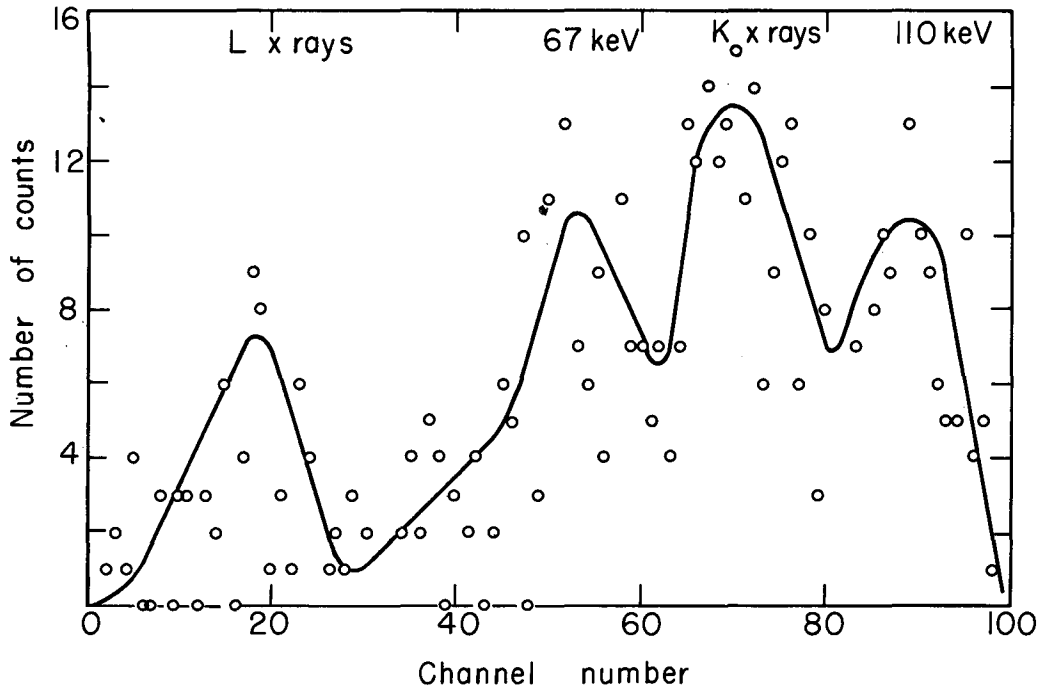
Fig. 6. Gamma spectrum in coincidence with  $\alpha_{65}$  of  $\text{Pa}^{227}$ .



a conversion coefficient of 0.35 for this transition. The theoretical conversion coefficients of E1(0.4) and M1(11) suggest clearly an E1 nature for this transition.

d. 110-keV state. Two  $\gamma$  rays of energies 67 and 110 keV and K x rays were found to depopulate this level as shown in Fig. 7. The curve drawn through the badly scattered experimental points is influenced by the  $\alpha$ -particle energies and the expected  $\gamma$  transitions. The intensities of the photons were calculated to be 14.5% of 67 keV and 25.5% of 110 keV per  $\alpha$  particle populating this state. The calculated conversion coefficients suggested strongly that the transitions are E1 in nature. The decay of this state to the two members of the ground-state rotational band is of particular interest. The relative intensities of the two E1  $\gamma$  rays, when considered with the E1 deexcitation of the 65-keV state to the ground state, suggests the possible presence of a second rotational band based on the 65-keV state with the second member at 110 keV. The parity of such a rotational band should be opposite to that of the ground-state band.

The amount of K x rays in coincidence was enough to account for the intensity of this alpha group, but the calculated K-conversion coefficient was much higher than the theoretical value of 0.3. This excess of observed K x rays may be attributed to an admixture of some M2 transition that also has an estimated half life comparable to the 1- $\mu$ sec resolving time of the coincidence equipment. Calculations indicate that such an admixture must consist of equal amounts of E1 and M2 transitions, which does not seem reasonable. Another explanation might involve an anomalously high E1 conversion coefficient. Such anomalous dipole transitions were reported earlier by Vartapetian<sup>11</sup> and Asaro et al.,<sup>12</sup> and the theoretical treatments for the retardation were given by Church and Wenéser,<sup>13</sup> Nilsson and Rasmussen,<sup>14</sup> and Kramer and Nilsson.<sup>15</sup> However, the competition of these interband dipole transitions with the enhanced intraband quadrupole transitions suggests that the life times involved are comparable and thus makes the anomalous E1 explanation unlikely. Also the possible presence of another unresolved, highly converted



MU-30102

Fig. 7. Gamma spectrum in coincidence with  $\alpha_{110}$  of  $\text{Pa}^{227}$ .

transition cannot be ruled out. This will be discussed later in further detail.

The intensities of other alpha groups are too low to conduct the coincidence work with the presently available experimental arrangement.

#### 4. Interpretation of Levels

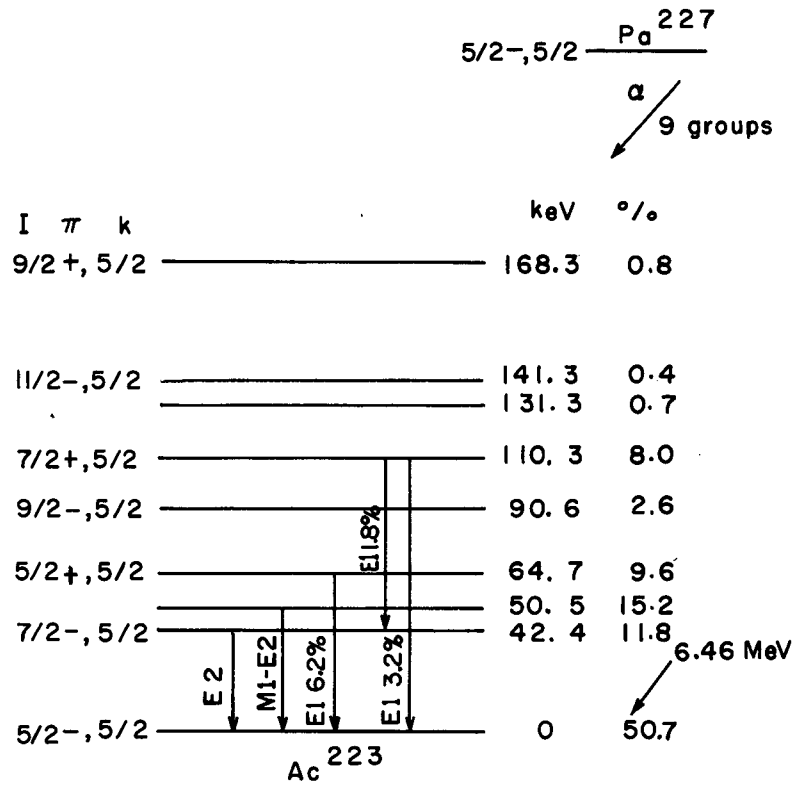
The decay scheme represented in Fig. 8 is derived from the data presented so far. Among the actinide elements, where the evidence for permanent deformation is good, there are at least five examples of rotational bands based on  $I=K=5/2$  that have been identified in which the spacings between the first two members have a characteristic energy of about 45 keV. For  $\text{Pa}^{227}$ , the observed 42-keV E2 transition points strongly to the conclusion that  $\text{Ac}^{223}$  belongs to this group. The energies of the members of a rotational band can be calculated according to the Bohr-Mottelson collective model,<sup>2</sup> where the energy,  $E_I$ , of a member of spin  $I$  is given by the simple expression

$$E_I = \frac{\hbar^2}{2\mathfrak{I}} [I(I+1) - I_0(I_0+1)], \quad (1)$$

where  $\mathfrak{I}$  is the effective moment of inertia and  $I_0$  is the spin of the lowest member. [In the case of  $I=1/2$ , the additional term  $\Delta E = \frac{\hbar^2}{2\mathfrak{I}} a(-)^{I+1/2} (I+1/2)$  should be added to the simple formula where  $a$ , the decoupling parameter, is a constant for each band.] In Eq. (1)  $I_0$  also represents the  $K$  quantum number, and for an odd-mass nucleus the sequence of spins in the band is  $I_0, I_0+1, I_0+2$ , etc.

The two levels observed at 90.6 and 141.3 keV are interpreted as the higher members of a rotational band based on the ground state of spin  $5/2$  with the first excited level at 42.4 keV. The agreement between the calculated and experimental energies is more convincing on the inclusion of a second-order term of the form  $BI^2(I+1)^2$  to the simple expression given by Eq. (1) (see Table III).

In odd-mass alpha emitters the decay to the unhindered or "favored" rotational band, where the odd nucleon of the daughter



MU-30098

Fig. 8. Decay scheme of  $\text{Pa}^{227}$  (present work).

Table III. Favored alpha decay to  $K=5/2$ -rotational band in  $\text{Ac}^{223}$ .

Spin of state	Excited-state energy (keV)			Relative intensity	
	Exp.	Theo.		Exp.	Theo.
		Simple	Second-order term $BI^2(I+1)^2$		
5/2	0	(0) <sup>a</sup>	(0) <sup>b</sup>	(100)	(100) <sup>c</sup>
7/2	42.4	(42.4) <sup>a</sup>	(42.4) <sup>b</sup>	23.0	22.0
9/2	90.6	96.9	(90.6) <sup>b</sup>	5.3	6.3
11/2	141.3	163.6	140.9	0.8	0.9

a.  $\hbar^2/2\mathcal{I}$  6.07 keV  
 b.  $\hbar^2/2\mathcal{I}$  7.0 keV, B = -0.04 keV  
 c.  $C_0 = 1.0$   $C_2 = 0.88$   $C_4 = 0.15$

remains in the same intrinsic state as the parent, was shown to be similar to the decay of the even-even nuclei to the ground-state rotational band.<sup>16</sup> A relationship has been developed by Bohr, Froman, and Mottelson for the calculation of the transition probabilities in such cases to the various members of the rotational band, represented in the form

$$P = P_0(Z, E) \sum_L C_L \langle I_i L K_f O | I_i L I_f K_f \rangle^2. \quad (2)$$

In the above expression,  $P_0(Z, E)$  represents a barrier penetration factor depending on the atomic number of the decaying nucleus and the energy of the outgoing  $\alpha$  particle, and is calculated from the one-body theory of alpha decay. The squared terms are the vector-addition coefficients for the distribution of various alpha waves and the  $C_L$ 's are the reciprocals of the hindrance factors of the states populated by alpha waves of angular momentum  $L$ . The hindrance factor<sup>17</sup> of an alpha group is defined as the ratio of the experimental to the theoretically calculated partial half life and is considered a constant for an alpha wave of a given angular momentum. If the spin assignments of the ground-state rotational band are correct, the intensities of the various members can be calculated by using the hindrance factors of the  $0+$ ,  $2+$ , and  $4+$  states populated in the neighboring  $\text{Th}^{226}$  and  $\text{U}^{228}$  even-even nuclei. Table III shows the agreement between the calculated and experimental values.

The presence of a second rotational band of opposite parity is indicated, as we suggested, by the observed electric dipole transitions. The level spacings again correspond to an  $I_0 = K = 5/2$ . If the two states at 64.7 and 110.3 keV belong to a rotational band, then the other members of the band are expected at 168.8 and 240.4 keV. The alpha group observed at 168.3 keV could be one of them, and is therefore suggested as the third member of the band.

The members of a rotational band populated by alpha waves of odd angular momentum can have  $L$  values of 1, 3, 5... The  $K$  selection rules restrict the values to  $L \leq (K_f + K_i)$ , and for this case mean  $L = 1, 3, \text{ or } 5$ . The intensities of these members also can be

calculated by Expression (2) using the appropriate Clebsch-Gordan coefficients and hindrance factors. In the adjacent even-even nuclei, only the 1- states were observed; by utilizing these hindrance factors and by assuming that only alpha waves of  $L = 1$  and 3 populated the states, we used two of the three experimental values to calculate  $C_3$ . The intensity of the third member was compared with the calculated value. The calculations are shown in Table IV, and the agreement is seen to be poor. It is clear from the last column of the table that the observed intensity of the 110-keV state is much higher than the one calculated using the intensities of the other two members. This fact combined with the observation that more K x rays than can be explained are in coincidence with this state provides further support to the suggestion that there is an unresolved  $\alpha$  group at the same energy. This will be considered again under the identification of various levels.

The various energy levels populated in  $\text{Ac}^{223}$  were identified with the help of the Nilsson diagram for protons, as shown in Fig. 9. This diagram is based on Nilsson's calculations<sup>18</sup> of the effect of a spheroidal deformation on the shell-model energy levels. The deformation is expressed in terms of the parameter  $\delta$ , which is defined as  $(R_{\text{major}} - R_{\text{minor}})/R_{\text{average}}$ . For a spherical nucleus,  $\delta = 0$ , the energy levels correspond to those of the shell-model calculations. As the deformation increases, the shell-model levels split into a number of components each of which is doubly degenerate. These levels in a spheroidal well are identified by quantum numbers  $\Omega \pi [N n_z \Lambda \Sigma]$ , where  $\Omega$  is the projection of the particle angular momentum,  $j$ , on the nuclear symmetry axis and has the parity  $\pi$ ,  $N$  is the principal oscillator quantum number,  $n_z$  is the symmetry-axis oscillator quantum number, and  $\Lambda$  and  $\Sigma$  are the orbital and spin components of  $\Omega$  such that  $\Omega = \Lambda \pm \Sigma$  depending on "spin up" or "spin down" conditions. Because of the relation that exists between  $\Omega$ ,  $\Lambda$ , and  $\Sigma$ ,  $\Sigma$  is often omitted in the identification of a state. For the relatively low energy states we have  $\Omega = K = I_0$ , where  $I_0$  is the spin of the lowest member of a rotational band based on  $\Omega$ . These quantum numbers

Table IV. Alpha decay to  $K=5/2$  + rotational band in  $\text{Ac}^{223}$ .

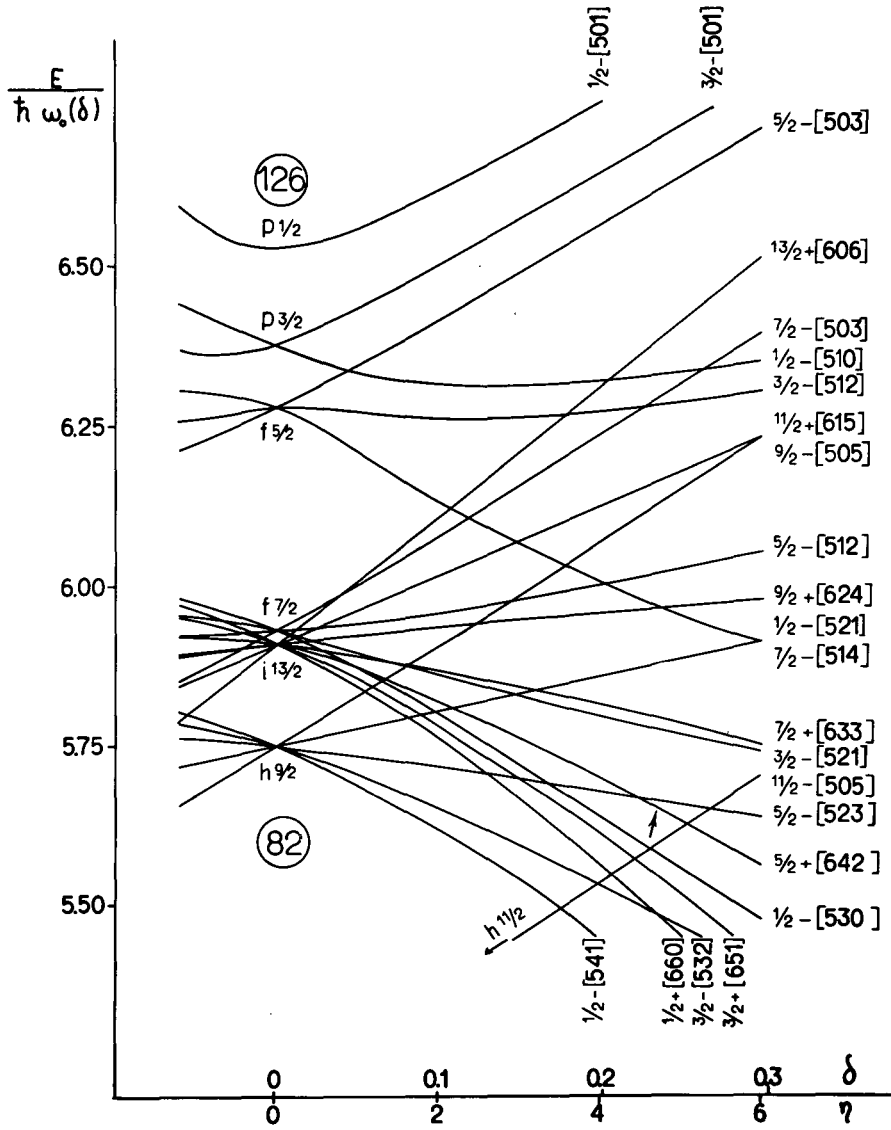
Spin of state	Excited-state energy (keV)		Relative intensity <sup>a</sup>		
	Exp.	Theo.	Exp.	Theo.	
5/2	64.7	(64.7) <sup>b</sup>	100	(100) <sup>c</sup>	(100) <sup>c</sup>
7/2	110.3	(110.3) <sup>b</sup>	84	(84) <sup>c</sup>	39
9/2	168.3	168.8	8.6	36.6	(8.6) <sup>c</sup>

a.  $C_1 = 0.173$ .

b. Experimental values used to calculate  $\hbar^2/2\mathfrak{I} = 6.15$  keV.

c. Experimental intensities used to calculate  $C_3$ .





MU-14829

Fig. 9. Nilsson diagram for 82 to 126 nucleons.

define the independent particle states in the limit of high nuclear deformation and are not applicable to spherical nuclei. Although the energy separations of Nilsson's calculations are only approximate, the order of filling of the states has proved very useful in correlating data pertaining to odd-mass nuclei. The state  $5/2$ -(642), indicated by a small arrow in Fig. 9, is believed to be the ground state of  $\text{Np}^{237}$  ( $Z=93$ ), but in the alpha decay of  $\text{Am}^{241}$  the population of this state is hindered to a great extent. The theoretical grounds for the "favored" ("unhindered") alpha decay, and its similarities to the decay of even-even nuclei, were first given by Bohr, Froman, and Mottelson.<sup>19</sup> The ground states of both the parent and the daughter in alpha decay may have the same configurations resulting from an appreciable change of deformation. This implies, as in the case of  $\text{U}^{233}$  decay, that the odd-particle state occupied in the daughter is vacated when the particle becomes paired. The ground state of proton number 91 is expected to be  $1/2$ -(530). The measured ground-state spin of  $3/2$  of  $\text{Pa}^{231}$  is supported by Coulomb-excitation studies,<sup>20</sup>  $\beta$ -decay<sup>21,22</sup> of  $\text{Th}^{231}$ , electron capture of  $\text{U}^{231}$ , and alpha decay<sup>23</sup> of  $\text{Np}^{235}$ . A spin of  $3/2$  for the ground state of  $\text{Pa}^{233}$  has been assigned from the alpha-decay studies<sup>24,25</sup> of  $\text{Np}^{237}$ . The ground states of both these isotopes have been suggested to be the  $I=3/2$  member of a rotational band based on  $I_0=K=1/2$ ,  $1/2$ -(530) state.<sup>26</sup> A spin of  $5/2$  for the ground state of  $\text{Pa}^{229}$  was proposed from its EC decay and from the population of levels in  $\text{Th}^{229}$ . In this region of deformation, the intrinsic state  $1/2$ -(530) crosses the state  $5/2$ -(523), and the ground state of  $\text{Pa}^{229}$  could have a spin of  $5/2$  provided it possesses a smaller nuclear deformation than  $\text{Pa}^{231}$ . This assumption is reasonable because of the decreased number of nucleons inside the nucleus, which brings the nucleus closer to the closed shell, thus resulting in a decrease of deformation.

It is now proposed that the ground states of both  $\text{Pa}^{227}$  and  $\text{Ac}^{223}$  have a spin of  $5/2$  and belong to the same intrinsic state  $5/2$ -(523). The decay is similar to that of  $\text{U}^{233}$  and implies a decrease in the deformation of the nucleus. A decrease in nuclear deformation

in this region is expected to lead to an increase in the value of the rotational constant,  $\hbar^2/2\mathcal{I}$ , as observed in the even-even cases. The absence of such an increase ( $\hbar^2/2\mathcal{I} = 6.07$  keV for the ground-state band) may be attributed to the interaction of this state with the neighboring states. It is seen from the Nilsson diagram that the possible states that can interact due to the Coriolis force are  $3/2-(532)$  and  $3/2-(521)$ , which are well separated in energy. However, the former state,  $3/2-(532)$ , has been assigned to the 27-keV level<sup>25</sup> in  $\text{Ac}^{227}$ , with a rotational band based on it. This state is not apparently populated in  $\text{Ac}^{223}$ . In the event of these states existing within a few hundred keV above the ground state of  $\text{Ac}^{223}$ , their interaction cannot account for the large difference of the rotational constant from those of the neighboring even-even  $\text{Th}^{226}$  and  $\text{U}^{228}$ . An additional effect of an unpaired nucleon on moments of inertia can arise from the decrease of pairing correlations (decrease in  $\Delta$ ) caused by the blocking of one orbital. This blocking effect as it relates to increasing moments of inertia has been discussed by Nilsson and Prior.<sup>26a</sup> It may be that the odd mass (at least odd proton) nuclei remain deformed longer than the even-even as one approaches the closed shells. This persistence of spheroidal deformation in odd-mass nuclei is supported by the interpretation<sup>27</sup> of the low-lying levels in  $\text{Fr}^{223}$  and  $\text{Fr}^{221}$  populated in the alpha decay of  $\text{Ac}^{227}$  and  $\text{Ac}^{225}$ , respectively, as members of rotational bands with large rotational constants and the apparent lack of rotational structure in the alpha decay of  $\text{Ac}^{223}$ . The presence of a permanent nuclear deformation justifies the use of the Nilsson diagram for the identification of the various levels. The need to consider the second-order term,  $-BI^2(I+1)^2$ , to match the calculated and experimental energies of the ground-state rotational band (see Table III) is reasonable in this region owing to the vibrational rotational interaction and the centrifugal stretching.

The assignment of spin  $5/2-$  for the ground state of  $\text{Ac}^{223}$  requires the second rotational band of opposite parity to be based on a  $5/2+$  state. The only such level available is the intrinsic state  $5/2+(642)$ . The observed hindrance factors do not permit such an

assignment. The low values of the hindrance factors and the decay of the 110-keV state to two members of the ground-state rotational band can be explained by assuming that both the bands have the same intrinsic state for the odd proton but with the core coupled to  $K = 0$ , odd parity, for the upper band. Core excited states with  $K = 0^-$  in nearby even-even nuclei lie higher in energy than our  $5/2^+$  band in  $\text{Ac}^{223}$ , but it may well be that coupling between the core excitation and odd proton motion could lower the energy of such a state. It is known that excited odd parity levels ( $1^-$ ,  $3^-$ , ...) come very low in energy for even-even nuclei of this region. There have been several theoretical explanations offered--one early explanation invokes the nature of a stable octupole deformation (pear-shaped nuclei);<sup>28</sup> another speaks of octupole vibrations about a spheroidal minimum; most recently Soloviev<sup>28a</sup> explained the low-lying odd parity levels in even-even nuclei on the basis of the superfluid model of the nucleus and the interaction of various two-quasi-particle states. The only known cases of odd-mass nuclei, where the octupole vibrational levels are believed to be populated, are the levels<sup>9, 26</sup> in  $\text{Ac}^{225}$  in the alpha decay of  $\text{Pa}^{229}$ , 665- and 690-keV levels<sup>29</sup> in  $\text{U}^{239}$ , and the 650-keV level<sup>30</sup> in  $\text{U}^{235}$ . The hindrance factor of the level in  $\text{U}^{235}$  was reported to be 75. For neighboring even-even nuclei  $\text{Ra}^{222, 224, 226}$  and  $\text{Th}^{226}$  the decay to  $1^-$  states exhibit low hindrance factors of less than four. These low hindrance factors, as also observed for the  $I = K = 5/2^+$  rotational band in  $\text{Ac}^{223}$ , are considered to be characteristic of octupole vibrations.

The presence of an unresolved highly converted 110-keV transition was suggested to explain the excess of the observed K x rays in coincidence with that level. The M1 nature of deexcitation of the 50-keV state provides more evidence for the assumption. The spin of this state is  $3/2$ ,  $5/2$ , or  $7/2$ . This could be the  $I = 3/2$  member of a rotational band based on the intrinsic state  $1/2^-(530)$  with the  $5/2$  and  $7/2$  members occurring at 80.8 and 110.3 keV, respectively. The rotational constant of this band would be 6.66 keV with a decoupling parameter,  $a$ , of -1.45 keV. The spin- $1/2$  member is then expected

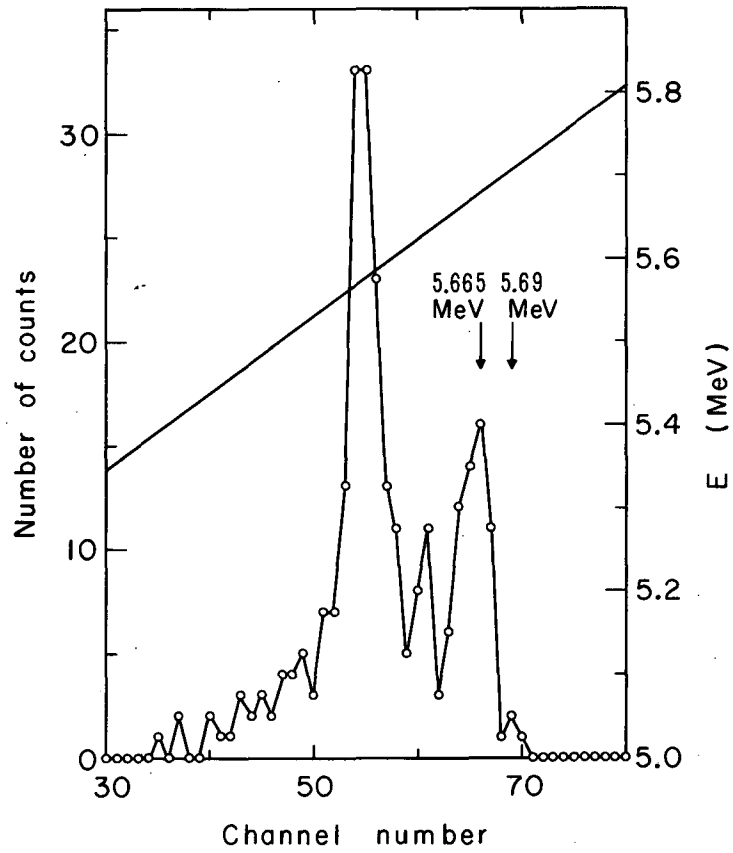
at about 60 keV and may remain unresolved from the adjacent intense  $\alpha$  groups. The intrinsic state under consideration is expected to be populated in the decay of nuclei of this region and has been identified as a rotational band at 330 keV in  $\text{Ac}^{227}$ . It should be emphasized, however, that the  $K = 1/2$  rotational band assignments are tentative and purely speculative and lack substantial evidence at this time.

### B. Alpha Decay of $\text{Pa}^{229}$

Protactinium (229) was first produced by Hyde and Studier,<sup>31</sup> who determined its half life of 1.5 d and observed an  $\alpha$ -particle energy of 5.66 MeV. Meinke et al.<sup>8</sup> confirmed the half life and measured the  $\alpha$ -particle energy to be 5.69 MeV. The alpha branching ratio was reported to be about 1%. Later work of Slater and Seaborg<sup>32</sup> and Asaro and Perlman<sup>33</sup> suggested an alpha branching of 0.25%. A decay scheme with two rotational bands was proposed by Hill<sup>9</sup> based on his studies of the fine structure of the alpha spectrum and the gamma spectrum associated with the alpha decay. To be consistent with previous work, it was proposed that the ground state was populated by  $\alpha$  particles of 5.665 MeV, leaving the observed  $\alpha$  group at 5.69 MeV unexplained. The present studies were undertaken to ascertain the ground state of  $\text{Ac}^{225}$  and to establish a decay scheme through  $\gamma$ -ray coincidence measurements with specific  $\alpha$ -particle energies.

#### 1. Ground State

It was reported by Stephens<sup>34</sup> that the  $\beta$  decay of  $\text{Ra}^{225}$  populated a 40-keV level in  $\text{Ac}^{225}$ , which became deexcited by the emission of an E1 gamma ray to the ground state. It was for this reason that the 5.69-MeV alpha group was not associated with the protactinium decay. In the present investigations, preliminary experiments were conducted to determine the alpha spectrum in coincidence with 40-keV  $\gamma$  rays. The samples of  $\text{Pa}^{229}$  used were the EC decay products of  $\text{U}^{229}$ , which assured isotopic purity. The results indicated (see Fig. 10) that 5.665- and 5.69-MeV  $\alpha$  particles were in



MU-32885

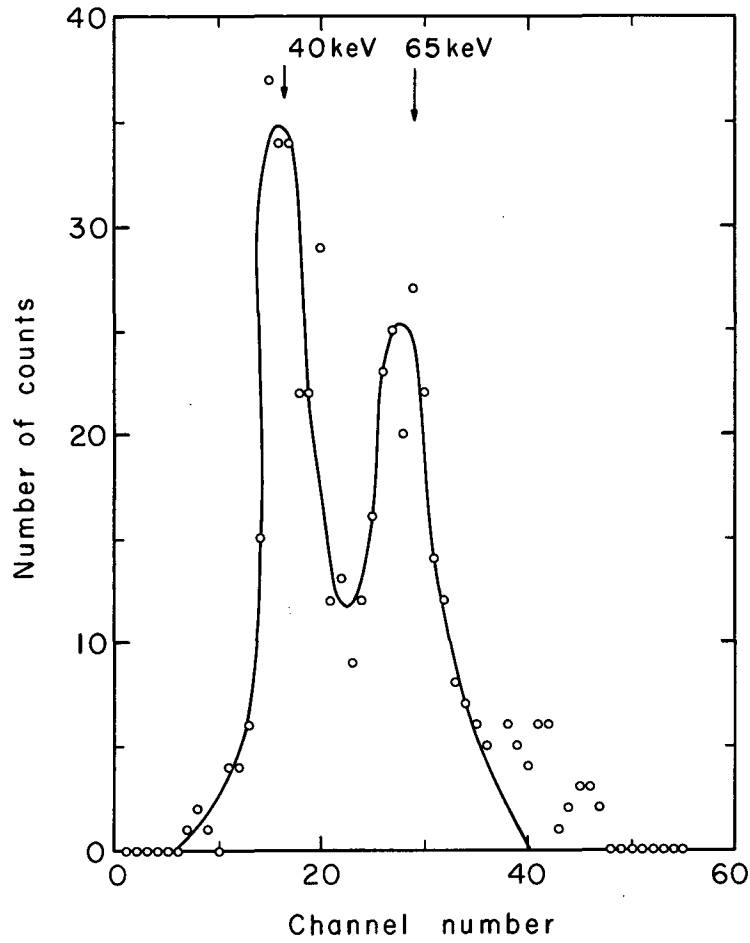
Fig. 10. Alpha spectrum of Pa<sup>229</sup> with  $\gamma$  rays of <50 keV energy.

coincidence; other  $\alpha$  particles of lower energies were also observed in coincidence.

The gamma spectrum in coincidence with  $\alpha$  particles of 5.665 MeV is shown in Figs. 11 and 12. The data for Fig. 11 were obtained with the equipment represented in Fig. 3 by following the procedure described in Sec. II. The coincident gamma spectra were determined by using a single-channel pulse-height analyzer to energy-discriminate  $\alpha$  particles (Fig. 2) and different resolving times of the equipment ranging from 250 nsec to 0.5 sec. The coincident gamma spectra contained both the  $\gamma$  rays (see Fig. 12) of 40 and 65 keV that decayed with the appropriate half life of approximately 1.5 d. We show that these  $\gamma$  rays deexcite the state independently. The parallel deexcitation of the level by the two  $\gamma$  rays indicates that the ground-state  $\alpha$ -particle energy of  $\text{Pa}^{229}$  is at least 5.73 MeV. The alpha spectrum of  $\text{Pa}^{229}$  determined by Hill was reexamined to find out whether the newly assigned ground state received any population. An alpha group of 5.73 MeV had been assigned as  $\text{Ac}_{\alpha 100}^{225}$ . A recalculation of the energy of this group indicated that it was 8 keV higher than the value reported by Asaro and Perlman.<sup>35</sup> This energy difference could be explained by assuming an alpha group of about 0.5% intensity at 5.73 MeV coming from the decay of  $\text{Pa}^{229}$ . This should be regarded as an upper limit. It is presently believed that the ground state of  $\text{Ac}^{225}$  is populated by 5.73-MeV  $\alpha$  particles from  $\text{Pa}^{229}$ ; the excitation energies of the various levels represented in Table VII and the decay scheme (Fig. 18) are based on this ground state.

## 2. Gamma Rays

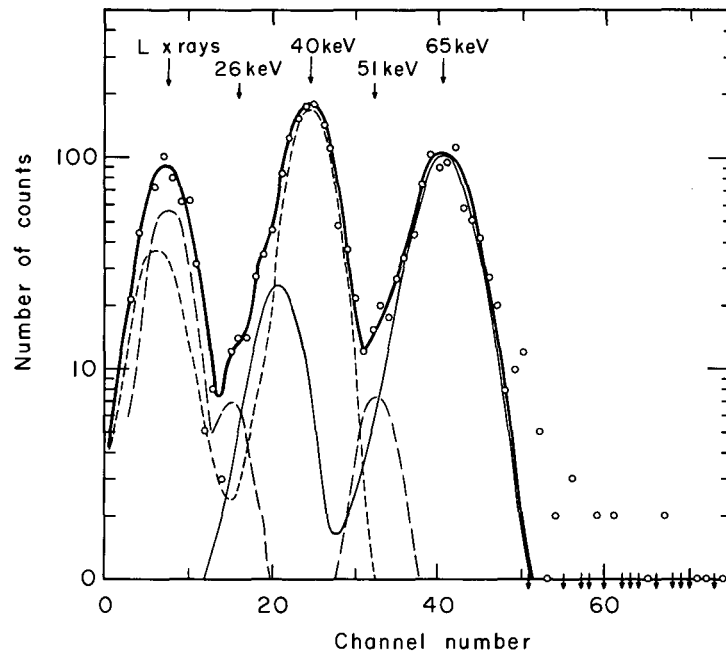
Gamma rays of energies 40(10%), 69(5%), 81(2%), 92(16%), 107(5%), and 120(2%) keV were reported<sup>9</sup> to accompany the alpha decay of  $\text{Pa}^{229}$ . The gamma spectra in coincidence with some of the alpha groups populated in the decay are presented in Figs. 13, 14, and 15. These spectra were obtained by a two-dimensional analysis, as described in Sec. II. These spectra will be described under each  $\alpha$ -particle energy populating the state. The alpha spectrum of the sample recorded during the experiment is shown in Fig. 16.



MU-32886

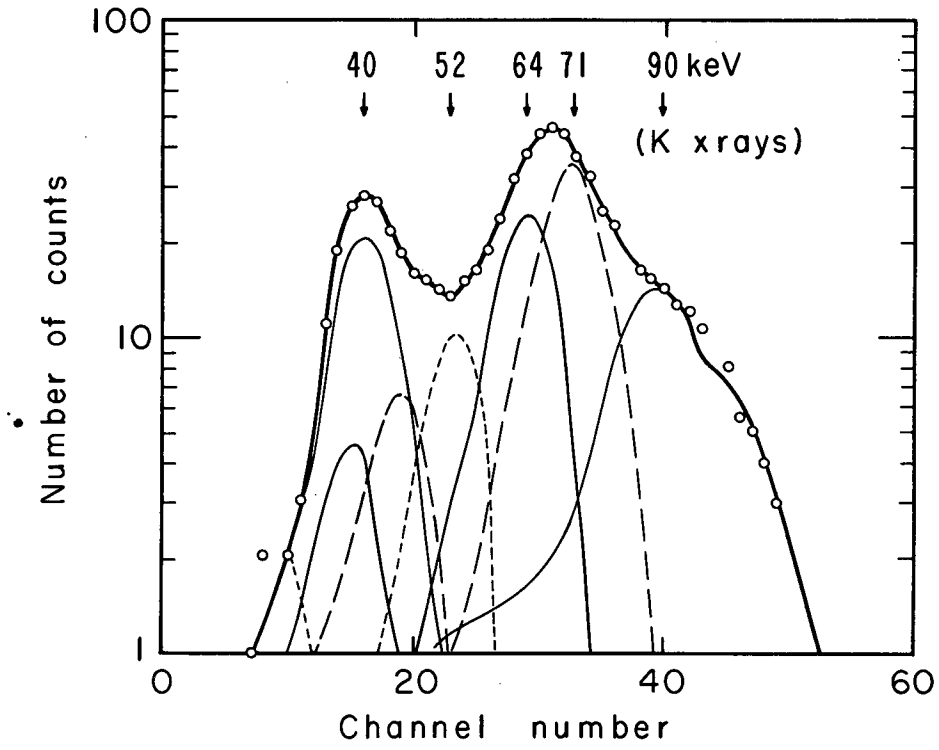
Fig. 11. Gamma spectrum in coincidence with 5.665-MeV  $\alpha$  particles of  $\text{Pa}^{229}$ , with two-dimensional analysis (resolving time 0.5 sec).





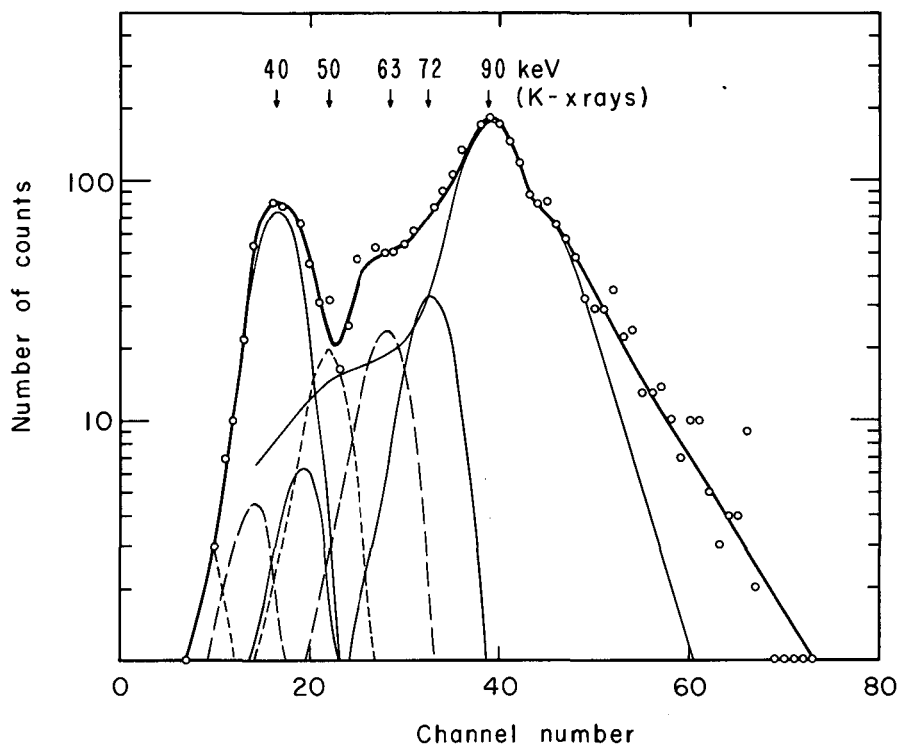
MU-32887

Fig. 12. Gamma spectrum in coincidence with 5.665-MeV  $\alpha$  particles of  $\text{Pa}^{229}$  (resolving time 250 nsec).



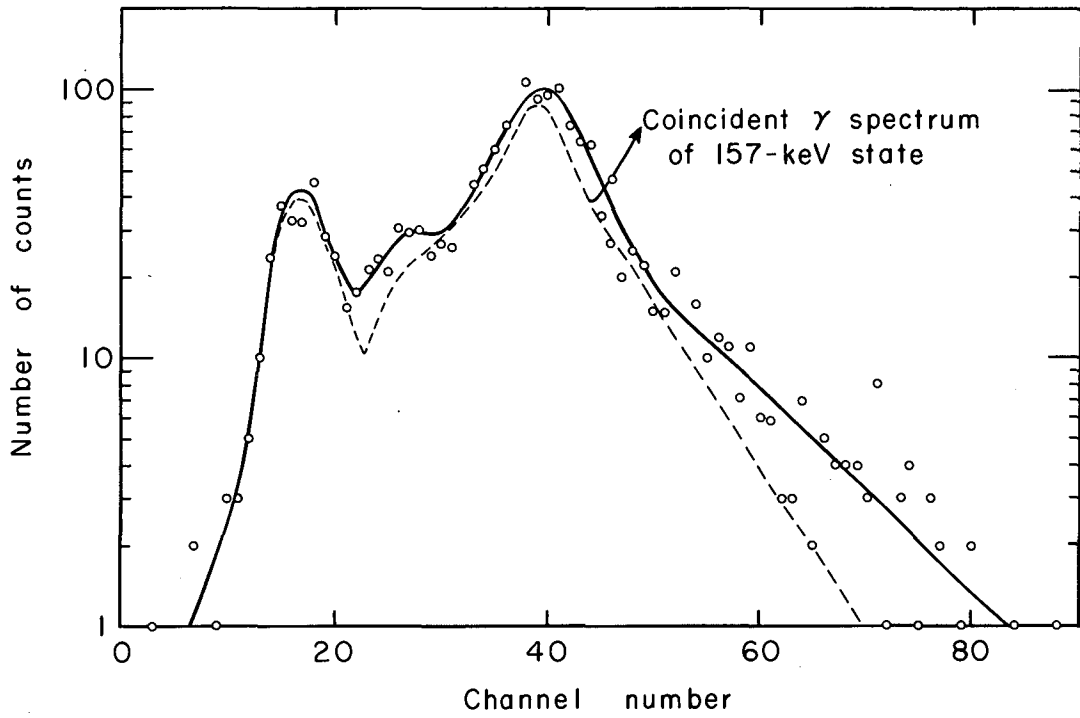
MU-32888

Fig. 13. Gamma spectrum in coincidence with (105 + 121)-keV alpha groups of Pa<sup>229</sup>.



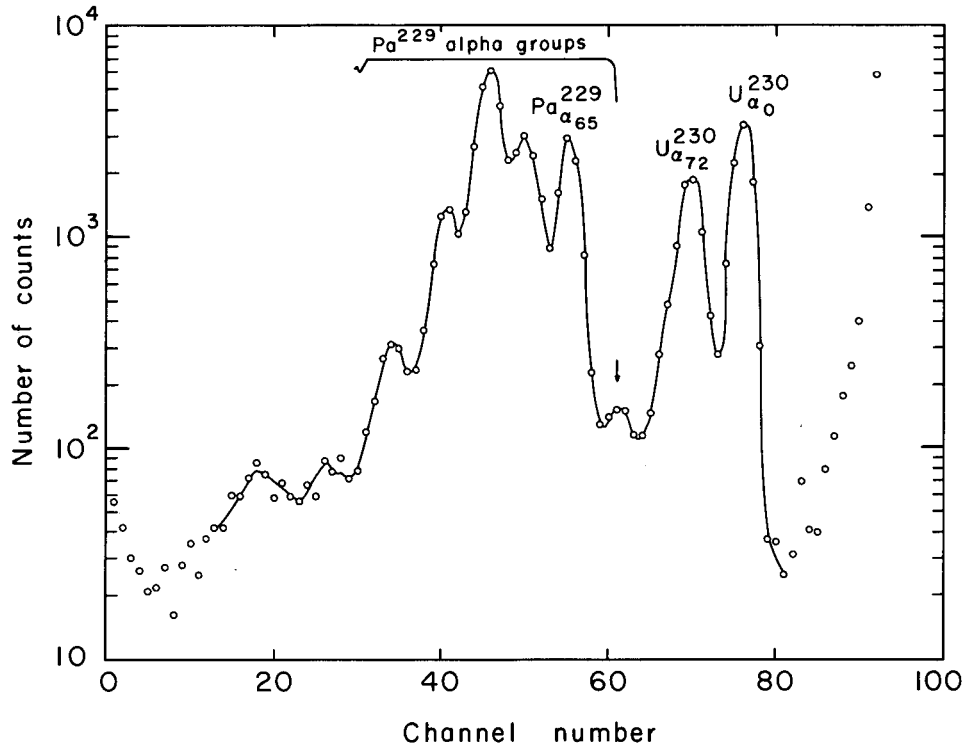
MU-32889

Fig. 14. Gamma spectrum in coincidence with alpha groups at 157 keV in  $\text{Ac}^{225}$ .



MU.32890

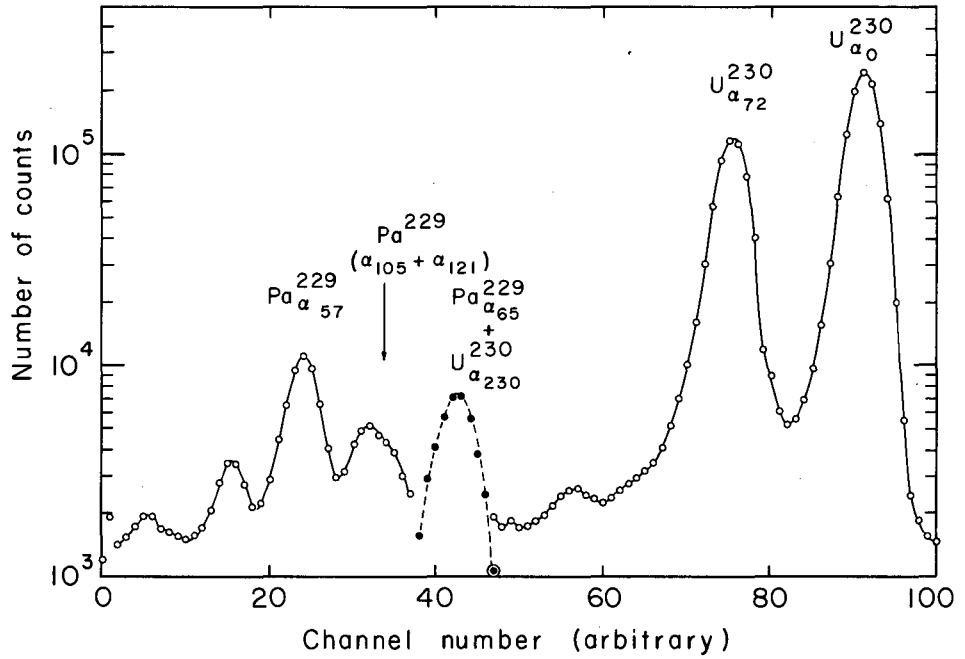
Fig. 15. Gamma spectrum in coincidence with  $\alpha_{201}$  of  $\text{Pa}^{229}$ .



MU-32891

Fig. 16. Alpha spectrum of Pa<sup>229</sup> used for the two-dimensional analysis.

a. 5.665-MeV  $\alpha$  particles. These  $\alpha$  particles were previously believed to populate the ground state. In the present investigations the gamma spectrum in coincidence with  $\alpha$  particles of this energy was studied extensively and repeatedly. Two prominent rays of 40 and 65 keV were observed in coincidence. The relative intensities of the two  $\gamma$  rays were always found to be the same, with the 65-keV being 66% of the 40-keV  $\gamma$  ray. The accurate determination of these  $\gamma$ -ray intensities was made difficult by the presence of two alpha groups from  $U^{230}$  of 0.7% intensity at 5.66 MeV. The 72-keV  $\gamma$  ray and the K x rays of the  $U^{230}$  family, whose amount increased rapidly by the decay of  $Pa^{230}$ , influenced the intensity of the 65-keV  $\gamma$  ray. The low-energy scattering from the  $U^{230}$   $\alpha$  groups also interfered with the determination of the number of alpha gates. The intensities of the  $\gamma$  rays were determined in the following manner: The gamma spectrum in coincidence with the alpha groups of  $U^{230}$  falling within the gate was determined after the complete decay of  $Pa^{229}$  and subtracted from the total coincident gamma spectrum by normalizing the 150-keV  $\gamma$  ray of  $U^{230}$ . The graphical subtraction gave the true gamma spectrum (Fig. 12) in coincidence with 5.665-MeV  $\alpha$  particles from  $Pa^{229}$ , which was then resolved into various  $\gamma$  rays by using standard peak shapes. The number of gates of  $Pa^{229}$  was determined by using Fig. 17, in which the full circles represent the gate region. The number of gates caused by the alpha groups of  $U^{230}$  (0.7%) was calculated from the ground-state group (67%) and was subtracted from the total number of gates. Within the gate region, the background caused by the low-energy scattering from alpha groups of higher energy, was also subtracted. The true alpha-gate number was also calculated from the intensity of the  $Pa_{a 157}^{229}$  (36.6%) alpha group at 5.575 MeV. The intensities of the 40- and 65-keV gamma rays were calculated to be  $18 \pm 2.5\%$  and  $12 \pm 3\%$ , respectively, of this alpha group. The graphical resolution of Fig. 12 into various  $\gamma$  rays indicated the presence of a  $\gamma$  ray of approximately 51 keV in an intensity of about 1% and possibly another  $\gamma$  ray of approximately 26 keV in an intensity of about 0.4% of this alpha group.



MU-32892

Fig. 17. Alpha spectrum of  $\text{Pa}^{229}$  for the intensity determination of 40- and 65-keV  $\gamma$  rays (full circles represent gate region).

b. The 5.625- and 5.610-MeV alpha groups. These two alpha groups could not be resolved with the experimental arrangement and are therefore considered together. The alpha-gate region used for the determination of the coincident gamma spectrum included all the  $\alpha$  particles populating the 105-keV level and approximately 70% of those populating the 121-keV level. This means that the gate region consisted of about equal amounts of  $\alpha$  particles populating the two states. In Fig. 13 we show the coincident gamma spectrum which has been resolved into a K x-ray peak and  $\gamma$  rays of 40, 52, 64, and 71 keV. The K x rays can arise from the 121-keV level, and possibly from the 105-keV level, if its excitation energy is above the K binding energy. In our present discussion, the latter state is considered to be under the K edge. The intensities of the  $\gamma$  rays per alpha gate (consisting of equal amounts of  $\alpha$  particles populating the two states) are shown in Table V.

Table V. Gamma rays in coincidence with  $\alpha$  particles leading to 105-keV and 121-keV states.

Energy of gamma ray (keV)	Intensity <sup>a</sup> (per alpha gate)	Multipolarity
40	13	---
51	5	---
64	13	---
71	21	E1
K x rays	10	---

a. The alpha gate consists of equal amounts of  $\alpha$  particles populating the two states.

c. The 5.575-MeV alpha group. This alpha group, denoted as  $\alpha_{157}$  in the decay scheme, was suggested to be the lowest member of a favored transition rotational band.<sup>9</sup> Owing to the limitations on the resolution of the alpha spectrum, this group is again considered with the adjacent groups at 146 and 172 keV, and their coincident gamma



spectrum is represented in Fig. 14. The gamma spectrum was resolved by considering the 90-keV energy region as a combination of a  $\gamma$  ray and K x rays. The intensity of any  $\gamma$  ray with energy  $>90$  keV, if present, was considered negligible. The intensities of the three gamma rays at 50, 63, and 72 keV energy were adjusted to account for the observed coincident gamma spectrum containing 40 keV gamma ray and K x rays. The calculated intensities of the various  $\gamma$  rays in coincidence with  $\alpha$  particles populating these levels are shown in Table VI. The energy spacings observed in the alpha spectrum were utilized in identifying the transitions responsible for the various  $\gamma$  rays.

Table VI. Gamma rays in coincidence with alpha particles leading to 142-, 157-, and 172-keV states.

Energy of gamma ray (ke V)	Intensity <sup>a</sup> (per alpha gate)
40	21
50	5
64	6
72	9
K x rays	84

a. Gates consist of all the  $\alpha$  particles populating the levels.

d. The 5.530-MeV alpha group. This alpha group was well resolved in the alpha spectrum, and the gamma spectrum in coincidence is shown in Fig. 15. It is seen from the coincident gamma spectrum that the decay of this level proceeds mostly ( $>70\%$ ) through the level at 157 keV. The possible presence of radiations at about 100 and 136 keV was indicated when the 157-keV coincident gamma spectrum was subtracted, normalizing the 40-keV peak in the two spectra. From the alpha spectrum, a possible explanation would be the presence of 96- and 136-keV gamma transitions. The intensities of these two  $\gamma$  rays were calculated to be about 10% and 20%, respectively.

### 3. Decay Scheme and Spin Assignments

The intensity of the alpha population to the 157-keV level indicated that it has a low hindrance factor (see Table VII). This type of unhindered decay is supposed to take place between the states of the same configuration. In the favored alpha decay of this nature, the whole rotational band is expected to be populated. The levels at 201, 259, and 329 keV were shown to be the higher members of such a rotational band ( $I_0 = K = 5/2$ ) from a consideration of their energy spacings and intensities.<sup>9, 36</sup> The levels at 121, 172, 237, and 317 keV in the present decay scheme (Fig. 18) were proposed by Hill<sup>9</sup> to constitute another rotational band based on the octupole vibrations of the favored band. If these assignments are correct, the lowest member of the favored band (157 keV) is expected to decay by E1 transitions to the members of the octupole band. The energy and peak shape of the radiation at 90 keV in Fig. 14 suggests strongly that it consists mostly of K x rays. The calculated intensity of K x rays (see Table VI) indicates that the decay of the levels at 157 keV are highly K converted; this points to the absence of any E1 transitions.

The presence of the 72-keV  $\gamma$  ray in Fig. 14 indicates that the levels at 157 keV decay partially through the levels at 105 and 121 keV. Only 2.5% of the observed 5% of the 50-keV gamma intensity can be accounted for by the decay through 105-, 121-keV levels. This is derived from the gamma spectrum in coincidence with these levels. The remaining 2.5% of the 50-keV  $\gamma$  ray can come either from the decay of the 172-keV level to the 121-keV state or from the decay of these states through the 51- or 65-keV levels, (or both).

The 64-keV  $\gamma$  ray of Fig. 14 can arise from the decay of the levels at 157 keV through the 65-keV level or the 105-, 121-keV combination. The observed intensity can be explained in both cases. If the decay proceeds through 105- and 121-keV levels about 6.5% of the observed 21% 40-keV  $\gamma$  ray can be explained, while a cascade through the 65-keV level explains about 9.6% of the 40-keV  $\gamma$  ray. In either case, the observed intensity of the 40-keV  $\gamma$  ray can be accounted for only by supposing a transition to the 40-keV state, a transition that

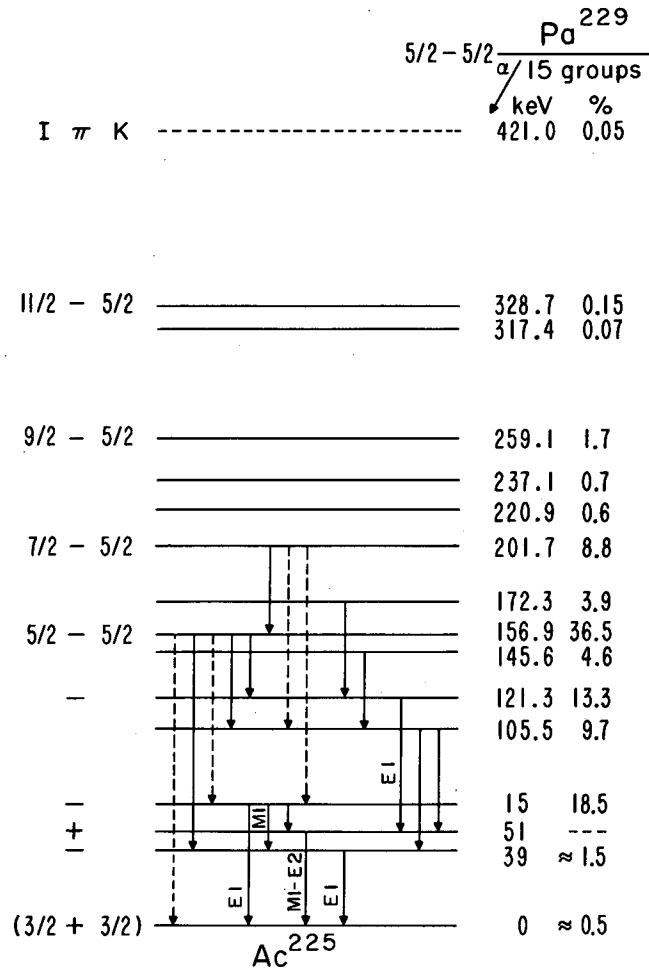
Table VII. Alpha groups of Pa<sup>229</sup>.

Alpha particle energy (MeV)	Excited state energy (keV)	Abundance <sup>a</sup> (%)	Hindrance factors <sup>b</sup>
5.73	0	0.5	1300 <sup>c</sup>
5.69	40	1.5	335 <sup>c</sup>
5.665	65	18.5	22
5.625	105.5	9.7	26.8
5.610	121.3	13.3	16.1
5.586	145.6	4.6	34
5.575	156.9	36.5	3.8
5.560	172.3	3.9	30
5.531	201.7	8.8	9
5.512	220.9	0.6	105
5.496	237.1	0.7	70
5.474	259.1	1.7	22.2
5.417	317.4	0.07	270
5.408	328.7	0.15	110
5.315	421.0	0.05	100

a. Values reported by Hill corrected for the addition of 5.73- and 5.69-MeV alpha groups.

b. Hindrance factors from reference 37.

c. Calculated as in reference 37.



MU-32893

Fig. 18. Decay scheme of  $\text{Pa}^{229}$ .

will have a maximum K conversion coefficient of 6 or 7 depending on the choice of the above-mentioned cascade.

The intensity of the observed K x rays in Fig. 14 suggests that they arise from the transitions depopulating the 157-keV level, leading to either 51- or 40-keV levels or the ground state. It is not presently known whether one or all of the transitions are taking place. However, it can be stated that at least one of the transitions should be M1 in nature to account for the K x rays. If the parity assignment of the ground state is correct, the choice would be in favor of a transition to the 40-keV level.

The decay of the 201-keV level is of particular interest because of its designation as the second member of the favored rotational band. The coincident gamma spectrum (Fig. 15) shows that the decay of this state proceeds mainly through the 157-keV level, which is consistent with the rotational assignments.

The 71-keV  $\gamma$  ray, in coincidence with  $\alpha$  particles populating the 105- and 121-keV levels (Fig. 13), is considered as coming from the decay of the 121-keV level to the 51-keV state. A maximum value of 1.3 for the conversion coefficient of the 71-keV transition can be calculated by assuming that equal amounts of  $\alpha$  particles leading to the 105- and 121-keV levels are present in the gates used for obtaining the coincident spectrum. The theoretical conversion coefficients for the transition are 0.26, 7.9, and 60 for E1, M1, and E2, respectively. The assumptions made in the calculation of the conversion coefficient are such that the actual value is smaller than 1.3, making the transition E1 in nature.

If we assume that all the K x rays observed in Fig. 13 come from the decay of the 121-keV level to the ground state, and use the intensity and theoretical conversion coefficient of the 71-keV gamma ray, a minimum value of 1.2 for the K conversion coefficient can be calculated for the 121-keV transition. The theoretical values for the various multipolarities are 0.2(E1), 0.3(E2), 7.0(M1) and (M2). It is not possible to make a choice for the multipolarity of the transition. If the 121-keV transition exists, the parity of the state indicates an M2 nature for the transition.

The intensity of the 52-keV  $\gamma$  ray in Fig. 13 cannot be explained by a cascade through the 51-keV level because of the highly converted nature of the decay of that level ( $\alpha = 44$ ). The decay of the 121-keV level to the 51-keV level can explain only 0.5% of the 5% intensity of the 52-keV  $\gamma$  ray, while the rest comes from the decay of the 105- and 121-keV levels to lower-lying states. However, as will be shown later, a cascade through the 65-keV level is not probable. The unresolved 54-keV  $\gamma$  ray arising from the decay of the 105-keV level to the 51-keV state can explain the 4.5% (9% with respect to one of the states of the combination) of the 52-keV  $\gamma$  ray. Such an explanation would give a maximum total conversion coefficient of 10 for the 54-keV transition, while the theoretical values are 0.54(E1), 17.7(M1), and 166(E2) which makes the choice of M1 reasonable for the transition.

The relative intensities of the 40- and 64-keV gamma rays in Fig. 13 suggest that a cascade through the 65-keV level is not probable. If such a cascade exists, the intensity of the 40-keV  $\gamma$  ray, contrary to the observation, should be higher than the intensity of the 65-keV  $\gamma$  ray. This indicated the presence of a 65-keV  $\gamma$  ray different from the one arising from the decay of the 65-keV level: the second 65-keV  $\gamma$  ray could come from the decay of the 105-keV level to the 40-keV state. The level at 105 keV, as seen earlier, also decays to the 51-keV state. With the presently available data, it is not possible to determine what portion of the 105-keV level decays to either the 40- or the 51-keV level.

The group populated by 5.665-MeV  $\alpha$  particles with an intensity of 19% is designated as the 65-keV level in the decay scheme shown in Fig. 18. The  $\gamma$  rays and their intensities that deexcite this state were discussed earlier under the specific alpha group. If the 40- and 65-keV  $\gamma$  rays are in cascade, the 65-keV  $\gamma$  ray should precede the 40-keV  $\gamma$  ray; this would be consistent with the  $\beta$  decay studies of  $\text{Ra}^{225}$  where the 40-keV state was shown to be the first excited level in  $\text{Ac}^{225}$  decaying to the ground state by an E1 transition.<sup>34</sup> By assuming a cascade of the two  $\gamma$  rays, a maximum total conversion

coefficient of 4 can be calculated for the 40-keV transition compared with the theoretical value of 1.1. On the other hand, a maximum total conversion coefficient of approximately 5 can be calculated for the 65-keV transition by assuming parallel transitions and by using the observed intensities and a conversion coefficient of 1.1 for the 40-keV  $\gamma$  ray. This turns out to be higher than the E1 value (0.4) and lower than the M1(11) and E2(80) values. If the two  $\gamma$  rays are in cascade, the coincidence effects are expected to produce in the coincident gamma spectrum (Fig. 12) a 105-keV energy  $\gamma$  ray of 10 counts peak height. The absence of a peak with the expected intensity indicates that the two transitions are in parallel. These two gamma rays, considered as parallel transitions and E1 in nature, will explain about 55% of the decay of the state, leaving approximately 45% of the decay to be explained by the 51-keV  $\gamma$  ray ( $\approx 1\%$  intensity). The total conversion coefficient of the parallel 51-keV transition can be calculated to be approximately 44 as compared with the theoretical values of 0.73, 22.7, and 200 for the E1, M1, and E2 transitions, respectively, suggesting an M1 nature for the transition with a small admixture of E2. The observed 51-keV  $\gamma$  ray requires the presence of a level at either 51 keV or 14 keV. The presence of a level at 51 keV, which presumably does not receive any alpha population, is preferred because of its usefulness in explaining the decay of the higher excited states. The 40-keV  $\gamma$  ray is considered to be the same one reported in the  $\beta$  decay of  $\text{Ra}^{225}$ , and the 40-keV first excited state is presently believed to be populated by  $\alpha$  particles of 5.69 MeV.

If all the  $\gamma$  rays in coincidence with the  $\alpha$  particles populating the 65-keV state are considered to be parallel transitions, the 65-keV  $\gamma$  ray explains about 18% of the decay of this state. The intensity of the 40-keV  $\gamma$  ray indicates that no more than 40% of the decay proceeds through that level. The intensity of the 26-keV  $\gamma$  ray ( $\approx 0.4\%$ ), considered as an M1 transition, explains all of the 40% decay that proceeds through the 40-keV level. The M1 assignment for the 26-keV transition is also consistent with the parities of the 40- and 65-keV states.

#### 4. Interpretation of Levels

Some of the levels represented in the decay scheme (Fig. 18) were identified with the help of the Nilsson's diagram shown in Fig. 9. The use of the diagram and the justification of its application were discussed earlier in this work.

The ground state of Pa<sup>229</sup> was suggested to have a spin of 5/2 based on its EC decay and the population of states in Th<sup>229</sup>.<sup>9</sup> It was identified by the Nilsson state 5/2-(523). The same assignment is given to the level at 157 keV in Ac<sup>225</sup> because of the favored nature of the alpha decay to this level. The rotational members with spins 7/2, 9/2, and 11/2 are identified at 201, 259, and 328 keV, respectively.

The ground state of Ac<sup>225</sup> is expected to be similar to either that of Ac<sup>223</sup> or Ac<sup>227</sup>. The Nilsson state assigned to the ground state of Ac<sup>223</sup> is identified as the 157-keV level in Ac<sup>225</sup>. The ground state of Ac<sup>225</sup> is therefore described by the Nilsson level 3/2+(651), which was assigned to the ground state of Ac<sup>227</sup>. The level at 27 keV in Ac<sup>227</sup> is tentatively assigned the intrinsic state 3/2-(532),<sup>25, 26</sup> which may also describe the 40-keV level in Ac<sup>225</sup> because of the similarities of the two levels that were already suggested.<sup>25</sup>

The parities of some of the levels indicated in the decay scheme are derived from the multipolarities of some of the observed transitions. Assignments of spins could not be made with the presently available data.

#### C. Alpha Decay of Actinium-223

Actinium-223 was first identified by Meinke<sup>8</sup> in the alpha decay of Pa<sup>227</sup>. It decays with a half life of 2.2 min and with an alpha branching of 99% emitting alpha particles of 6.64 MeV. The fine structure of the alpha spectrum was reported by Hill,<sup>9</sup> based on the magnetic analysis of alpha particles from Pa<sup>227</sup> sources. The alpha groups at 6.657, 6.643, and 6.561 MeV were assigned to the decay of Ac<sup>223</sup>. As reported earlier in this work, our original consideration that the alpha group at 6.52 MeV was the ground state in the decay of Pa<sup>227</sup>

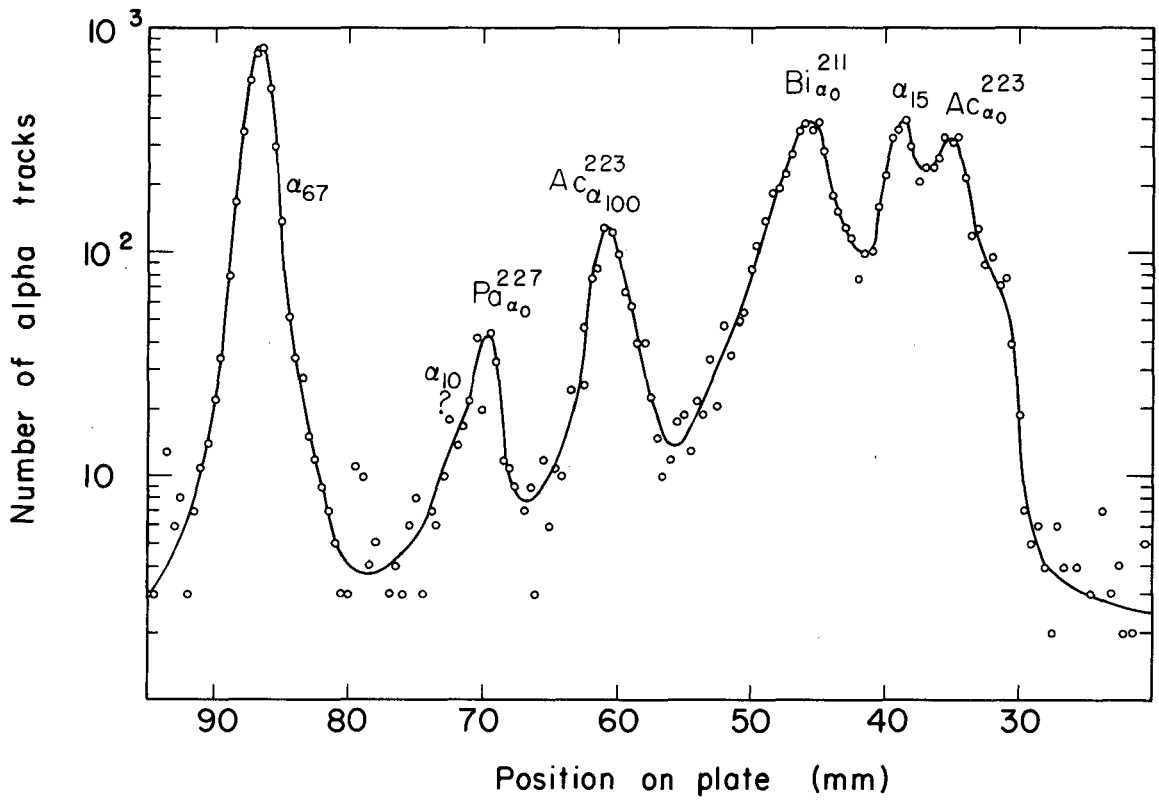


was not borne out, and a systematic study was undertaken with pure  $\text{Ac}^{223}$  samples isolated from its parent.

### 1. Alpha Spectrum

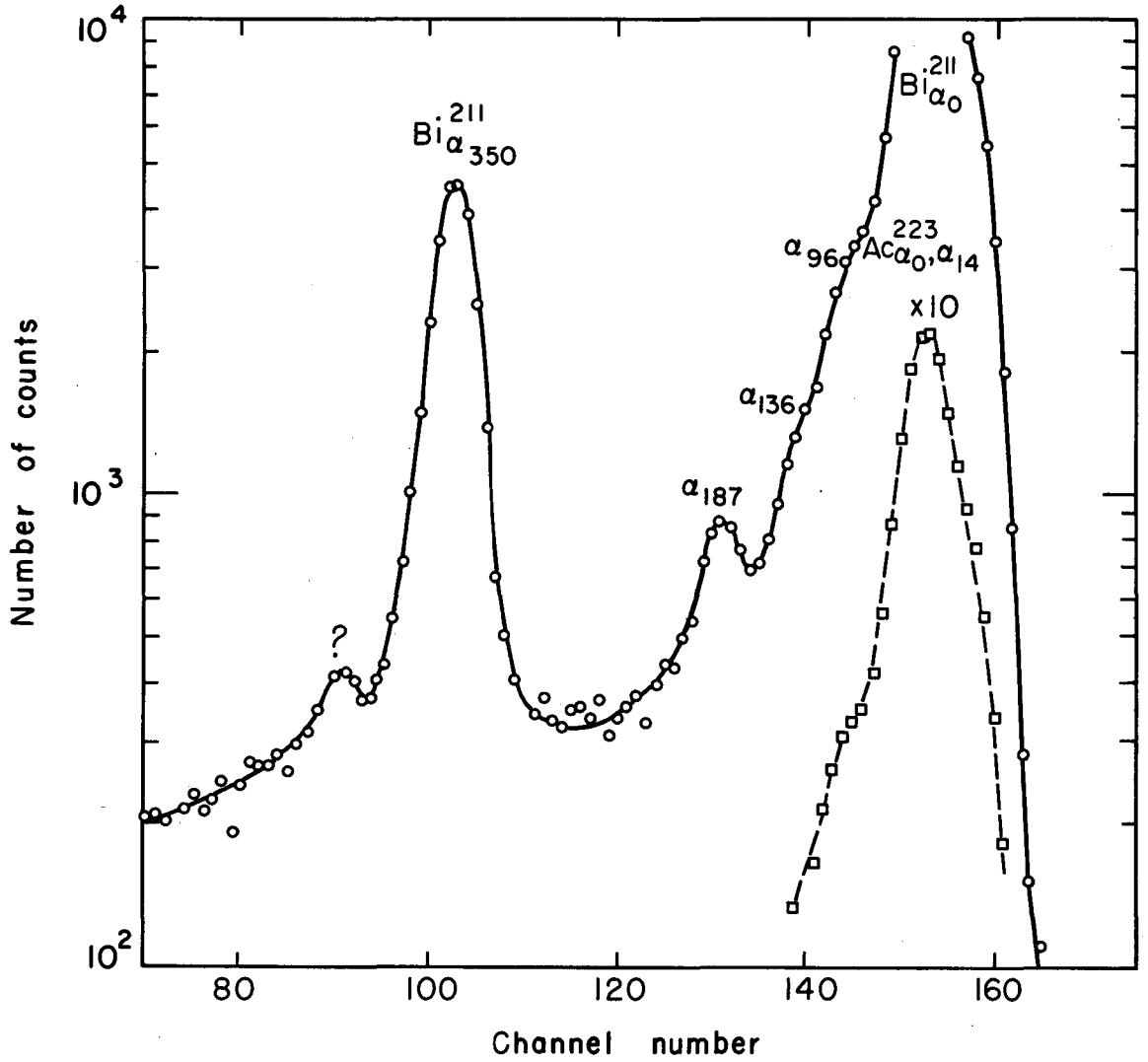
The region of the  $\alpha$  spectrum attributed to  $\text{Ac}^{223}$  by Hill is reproduced in Fig. 19. The  $\alpha$  spectrum that we obtained from pure  $\text{Ac}^{223}$  by using surface-barrier detectors is represented in Fig. 20. The samples were prepared by collecting recoils from  $\text{Pa}^{227}$  sources. The various  $\alpha$  groups are not well resolved in the latter spectrum because of the low-energy scattering from the higher-energy  $\alpha$  particles. However, the presence of an  $\alpha$  group denoted as  $\alpha_{136}$  at 6.52 MeV is very clear. In the alpha decay of  $\text{Bi}^{211}$  it was shown by Pilger<sup>5</sup> that in this energy region no levels greater than 0.1% in intensity were populated. The alpha group at 6.52 MeV, which evidently belongs to  $\text{Ac}^{223}$  or its daughters, is therefore assigned to  $\text{Ac}^{223}$ . This assignment derives further support from the  $\alpha$ -particle —  $\gamma$ -ray coincidence studies reported later.

The alpha group at 6.47 MeV in Fig. 20, denoted as  $\alpha_{190}$ , is of particular interest. The presence of this group, assigned also to the decay of  $\text{Ac}^{223}$ , was confirmed following repeated observations made with special care to avoid any contamination in the recoil samples of  $\text{Pa}^{227}$ , which also has an intense alpha group at about the same energy. The energy of the  $\alpha$  particle populating this state was determined to be  $6.470 \pm 0.005$  MeV, which is in agreement with the value determined from Fig. 12 based on the magnetic analysis of the  $\alpha$  particles. The presence of this group is also indicated in the alpha spectrum reported by Hill. Attempts to obtain the alpha spectrum of the recoils of  $\text{Pa}^{227}$  on the magnetic spectrograph were not successful because of the short half life. Figure 21 shows the alpha spectrum of  $\text{Ac}^{223}$  obtained on the magnetic spectrograph by using thin samples of  $\text{Pa}^{227}$ , and the intensities of the alpha groups are summarized in Table VIII.



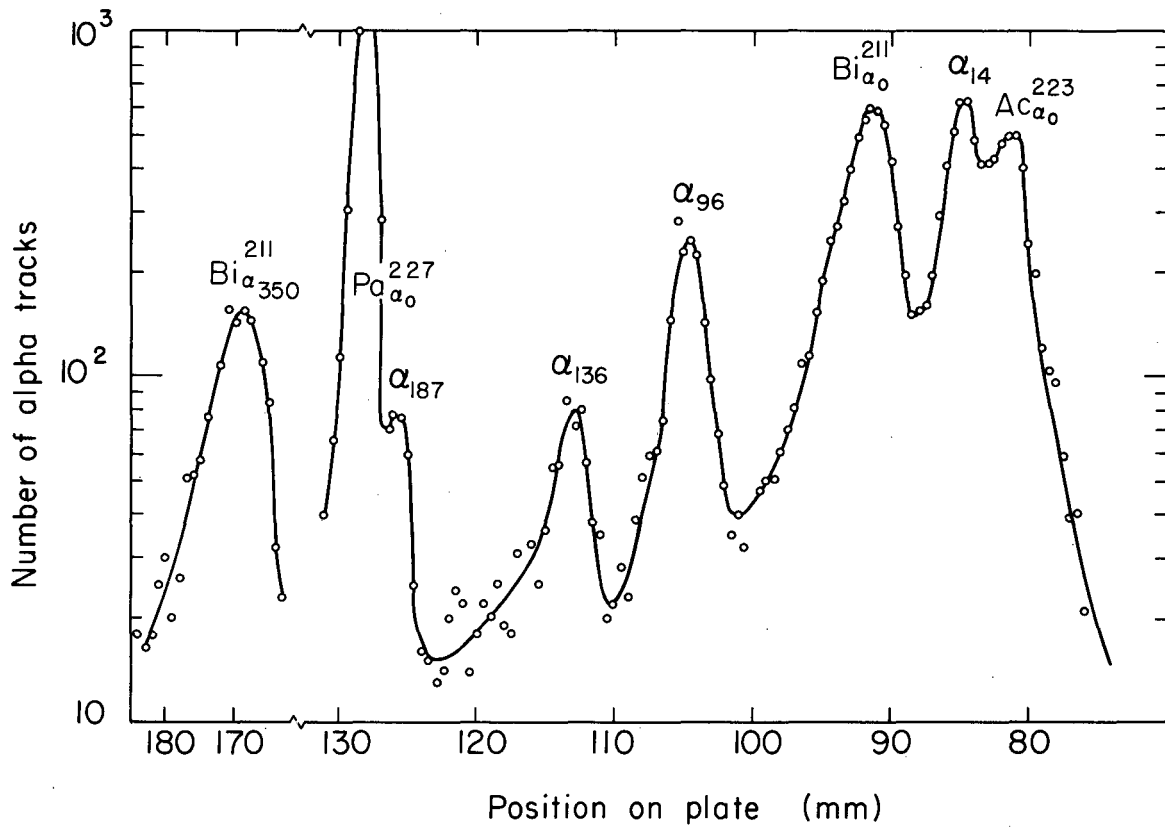
MUB-1742

Fig. 19. Alpha spectrum of  $Ac^{223}$  (assignments by Hill).



MUB-1740

Fig. 20. Alpha spectrum of recoils from  $\text{Pa}^{227}$  sources.



MUB-1741

Fig. 21. Alpha spectrum of Ac<sup>223</sup> and Bi<sup>211</sup>.

Table VIII. Alpha groups of Ac<sup>223</sup>.

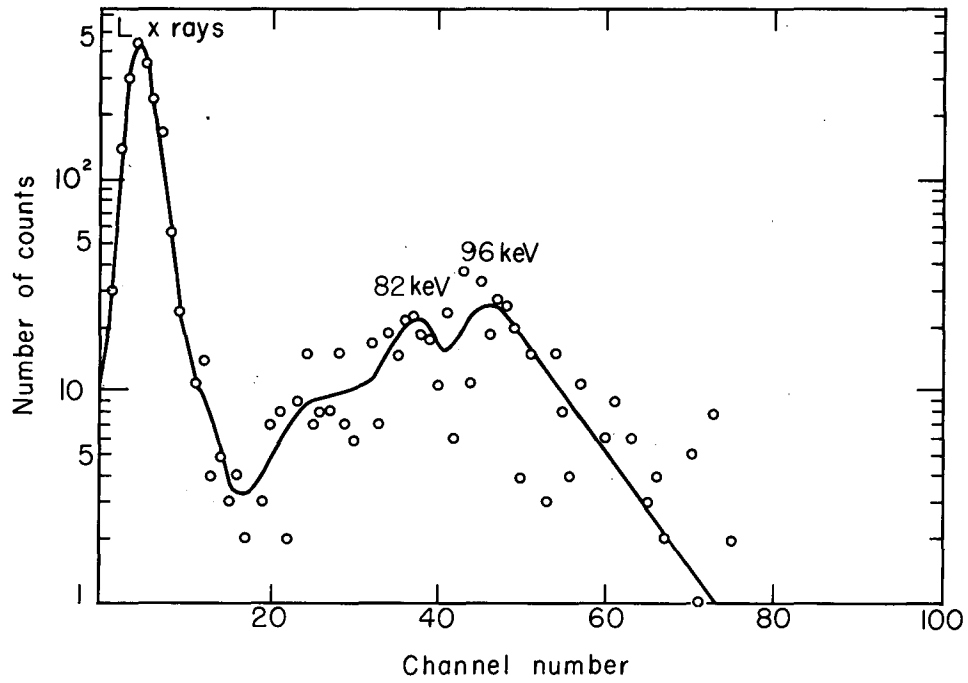
Alpha-particle energy (MeV)	Excited-state energy (keV)	Abundance (%)	Hindrance factor
6.56 <sub>7</sub>	0	37.5	7.9
6.64 <sub>3</sub>	15	42.1	8.0
6.56	98	13.3	10.6
6.52	136	3.8	25.2
6.47	185	3.2	6.3

## 2. Gamma Rays

The singles spectra of the  $\gamma$  rays from samples of Pa<sup>227</sup> recoils showed only one peak of 350 keV corresponding to the Bi<sup>211</sup> alpha decay. No other photons of measurable intensity were observed. Coincidences between  $\alpha$  particles from Ac<sup>223</sup> and  $\gamma$  rays were measured and the results are described below under each level.

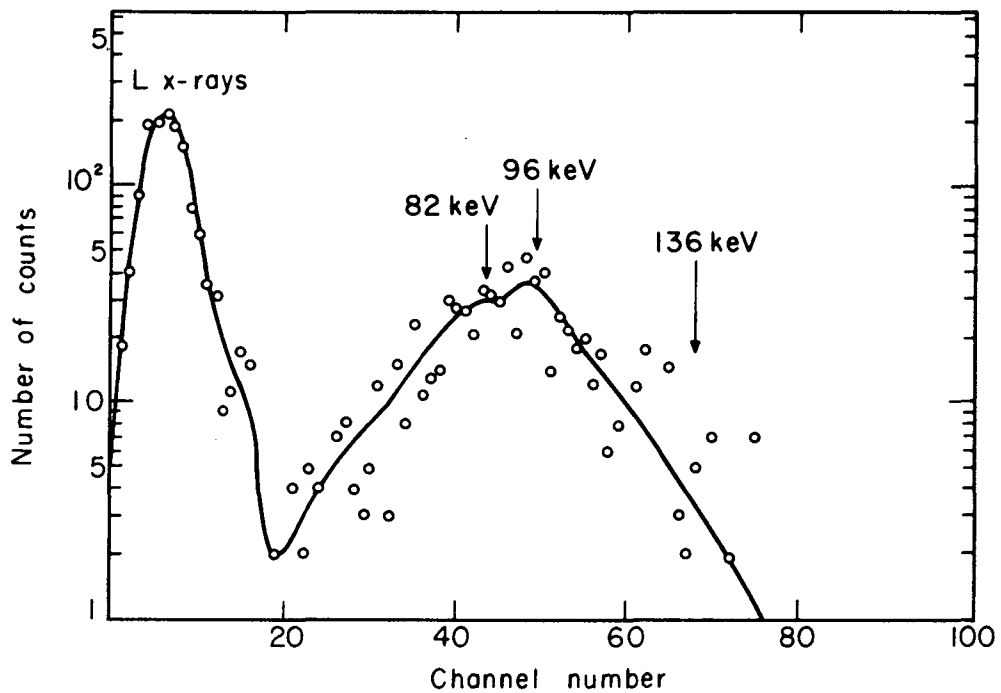
a. 96 keV state. The gamma spectrum in coincidence with the  $\alpha$  particles populating this state is shown in Fig. 22. The energy of this level being under the K edge of francium, the broad photon peak was considered complex and was resolved by utilizing independently determined peak shapes. The intensities of the two  $\gamma$  rays at 82 keV and 96 keV were calculated to be 0.014 and 0.02 photon, respectively, per  $\alpha$  particle populating this state. The total vacancies calculated from the observed L x rays, after we corrected for their absorption and assumed a fluorescence yield of 0.5, were just enough to account for the intensity of this group. The ratio of the vacancies to the total photon intensity was determined to be 26, which can be explained by assigning an E2 nature for both these transitions, assuming the theoretical conversion coefficients of Sliv and Band.<sup>10</sup>

b. 136 keV state. The gamma spectrum in coincidence with  $\alpha$  particles populating this level is presented in Fig. 23. It is evident from the coincident spectrum that the decay of this state proceeds through the 96-keV level. The ratio of the total vacancies to the



MU-30101

Fig. 22. Gamma spectrum in coincidence with  $\alpha_{96}$  of  $\text{Ac}^{223}$ .



MU-30100

Fig. 23. Gamma spectrum in coincidence with  $\alpha_{136}$  of  $\text{Ac}^{223}$ .

radiation in the region 80 keV to 100 keV was calculated to be 12 from the coincidence spectrum, which when compared with the value of 26 obtained in the deexcitation of the 96-keV level, suggests clearly the presence of francium K x rays that can only arise from a direct transition to the ground state or to the 14-keV state. The observed total vacancy photon ratio may be explained by assuming an additional 0.15 K vacancy per  $\alpha$  particle populating this level, which gives a K conversion coefficient of about 5, which makes the choice of M1 transition reasonable. In arriving at this assignment the 40-keV transition leading to the 96-keV level was considered as completely converted.

c. 187-keV state. The deexcitation of this level proceeds through the 96-keV level; any K x rays present under the peak observed in the energy range 80 keV to 100 keV can arise only from the K conversion of the cross-over transition to the ground. From the coincident gamma spectrum (Fig. 24), we calculated the ratios of the total vacancies to the radiation in the K x ray region and to the  $\gamma$  ray of about 170 keV. The values were 4.5 and  $\approx 100$ , respectively.

The low intensities of the various  $\gamma$  rays and the relatively large errors involved in their determination do not permit the unambiguous assignments of multiplicities to these transitions, but the tentative intensities and multiplicities are given in Table IX.

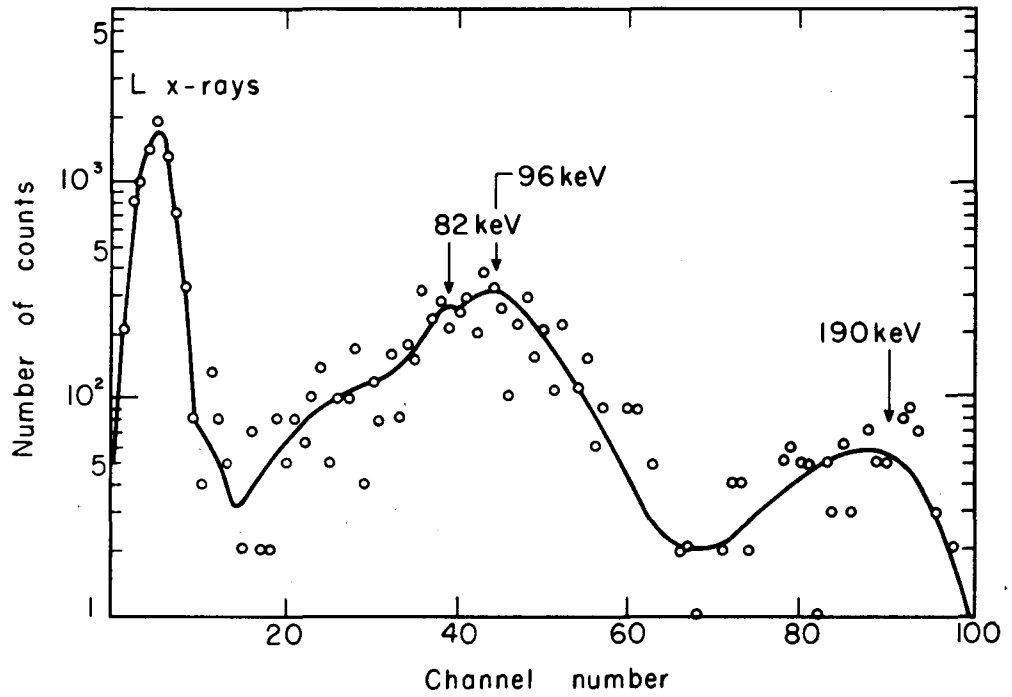
Table IX. Abundances of  $\gamma$  rays in the alpha decay of  $\text{Ac}^{223}$ .

Energy of level (keV)	Gamma-ray energy (keV)	Intensity per decay	Multiplicity
96	82	$2.3 \times 10^{-3}$	E 2
---	96	$2 \times 10^{-3}$	E 2
136	123	$< 5 \times 10^{-4}$	M 1
187	$\approx 170$	$< 8 \times 10^{-3}$	M 1

### 3. Decay Scheme and Interpretation of Levels

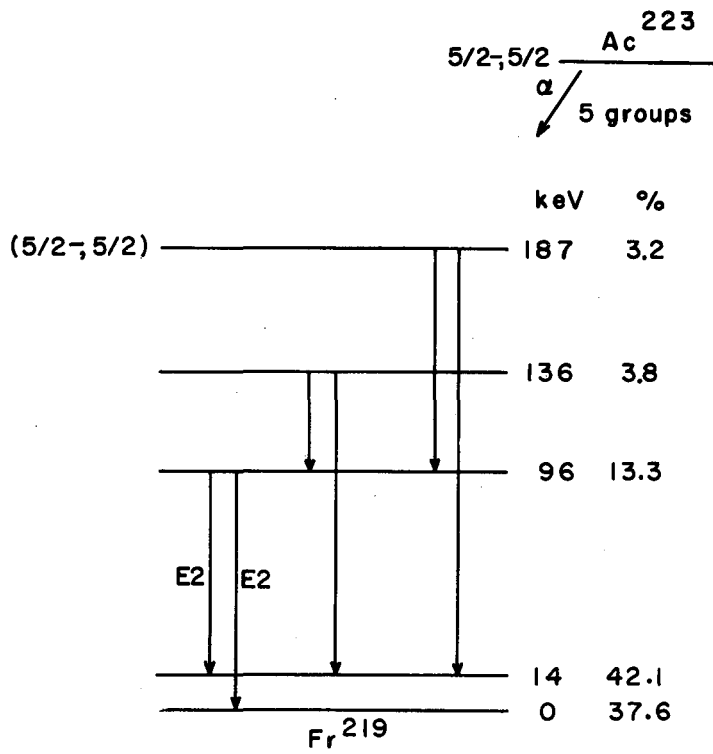
The decay scheme indicated in Fig. 25 is based on the information presented in this section. If the multiplicities suggested in the





MU.30103

Fig. 24. Gamma spectrum in coincidence with  $\alpha_{187}$  of  $\text{Ac}^{223}$ .



MU-30094

Fig. 25. Decay scheme of  $\text{Ac}^{223}$ .

table are correct then all the levels should belong to the same parity. The hindrance factor of the alpha group at 185 keV suggests the possible presence of favored decay to this state, in which case its spin and parity will be same as the ground states of both Pa<sup>227</sup> and Ac<sup>223</sup>, 5/2<sup>-</sup>(523). Any further identification of the levels is not possible at this time.

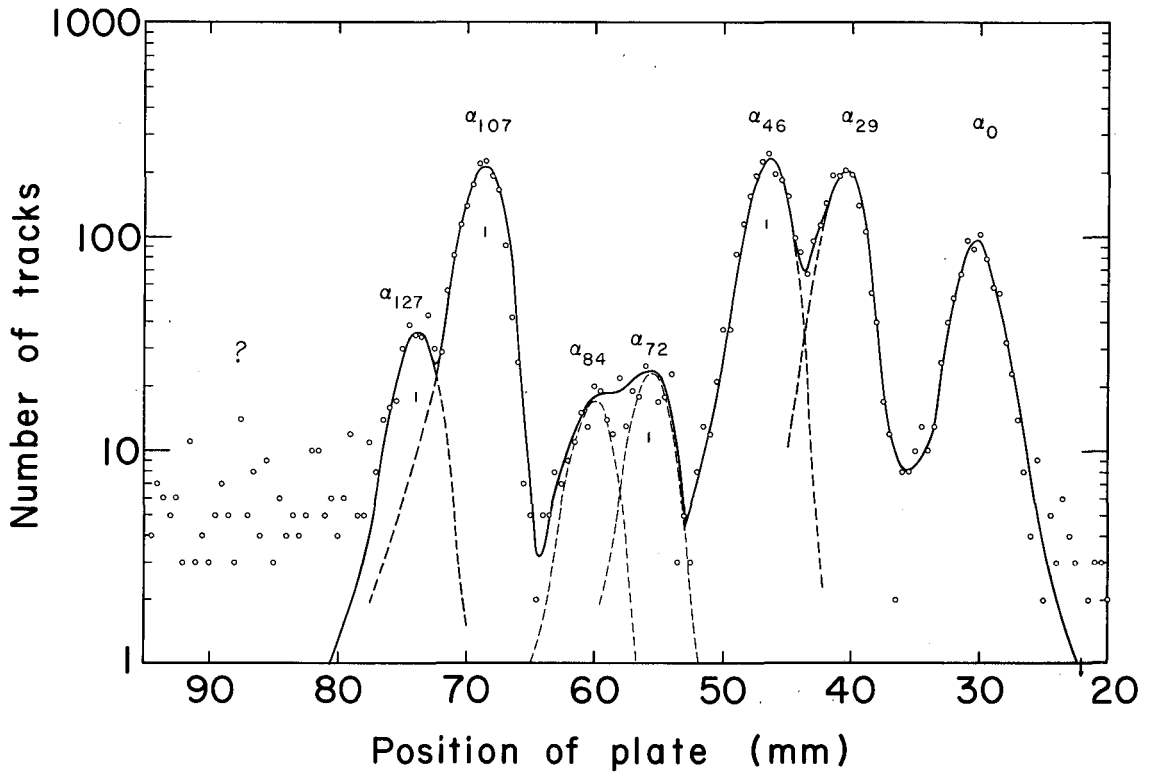
#### D. Other Experiments

The experiments reported in this section were all conducted with Pa<sup>231</sup> samples. Pa<sup>231</sup> is one of the natural alpha emitters, and a considerable amount of work has been done with this long-lived ( $T_{1/2} = 3.4 \times 10^4$  y) isotope. The alpha-decay fine structure of Pa<sup>231</sup> was first reported by Rosenblum,<sup>38</sup> who attributed six alpha groups for its alpha decay. It was later shown that the alpha spectrum was more complex than was first reported.

The conversion-electron studies following the alpha decay were more extensive;<sup>39,40,41</sup> this led to the conclusion that the alpha group observed at 29 keV consisted of more than one level. The half life of the 27-keV level that decays by an E1 transition to the ground state was determined to be 42.5 nsec and 37 nsec, from the  $\alpha$ - $\gamma$  and  $\gamma$ - $\gamma$  coincidence methods, respectively.

##### 1. Alpha Spectrum of Pa<sup>231</sup>

A portion of the alpha spectrum of Pa<sup>231</sup> obtained by means of the magnetic analysis of the  $\alpha$  particles is presented in Fig. 26. The sample used was 0.020 in. wide and had an activity of  $2 \times 10^5$  dis/min. The alpha groups at 71 and 84 keV were reported<sup>42</sup> as a single group of 76 keV. The energies of the two groups were determined relative to the 46 and 107-keV groups that were present on the same plate. The intensities of the two new groups were calculated to be approximately 1% and 1.5%, respectively. The intensities of the same groups were reported to be 0.5% and 1.4% in the work of Baranov, (et al.).<sup>26</sup> The scattered points at 90 mm in Fig. 25 were shown by them to constitute another group.



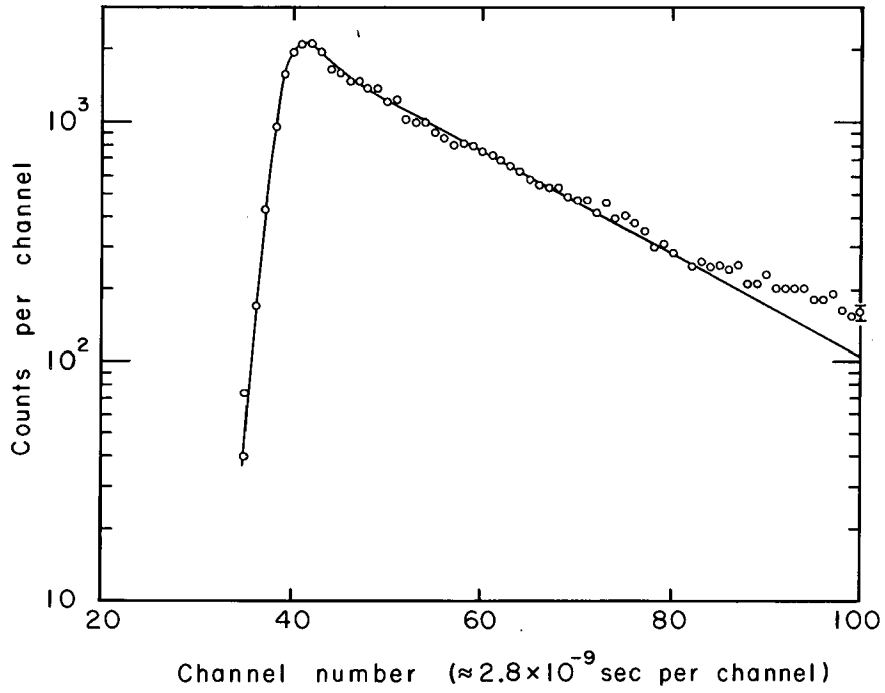
MUB-2284

Fig. 26. Part of the alpha spectrum of  $\text{Pa}^{231}$ .

## 2. Gamma-Gamma Coincidences

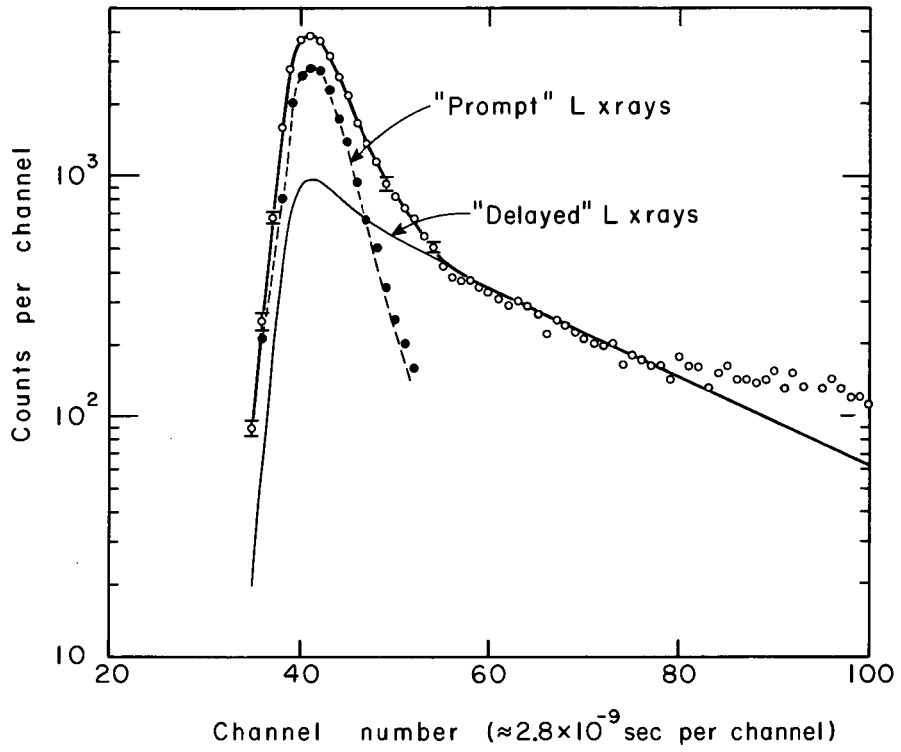
The conversion-electron spectrum given by Stephens<sup>43</sup> indicated two lines of 299 and 301 keV energy that were interpreted as conversion electrons accompanying the decay of the 329-keV to two states at 29 and 27 keV.<sup>42</sup> The present experiment is aimed at obtaining direct evidence for the two transitions by utilizing the fact that the 27-keV level has half life of about 40 nsec.

Part of the experimental arrangement consisted of a height-to-time converter (HTC). The working principle of the HTC is that the height of its output pulse is proportional to the time difference between the start and stop pulses. In the present experiment the stop pulses consisted of either the 27-keV  $\gamma$  rays or L x rays, and the start pulses were the 300-keV  $\gamma$  rays. The proper functioning of the equipment is seen in Fig. 27, from which half life of the 27-keV level is determined; the stop pulses used were the 27-keV  $\gamma$  rays obtained after the complete absorption of the L x rays. The half life of the 27-keV level, as determined from Fig. 27, was 42.5 nsec. Figure 28 was obtained in exactly the same way as Fig. 27, except for the important difference that L x rays were used as stop pulses instead of the 27-keV  $\gamma$  rays. If all the L x rays were to come from the 27-keV transition, both Figs. 27 and 28 would be identical. It can be seen from Fig. 27 that there are some "prompt" L x rays that can arise only from a fast transition following the 300-keV  $\gamma$  ray. The presence of the prompt and delayed L x rays shows clearly that the 329-keV level decays to two levels at about 29 keV, out of which one level decays promptly to the ground state. Baranov et al., from their studies of Pa<sup>231</sup>, reported that the 27- and 29-keV states received 2.4% and 20% of the population of the total alpha decay.<sup>25</sup>



MU-32894

Fig. 27. Time delay between 300- and 27-keV  $\gamma$  rays of  $\text{Pa}^{231}$ .



MU-32895

Fig. 28. Time delay between 300-keV  $\gamma$  rays and L x rays of  $\text{Pa}^{231}$ .

## ACKNOWLEDGMENTS

The author is indebted to the Lawrence Radiation Laboratory of the University of California for the facilities and support required for the study and to the department of Chemistry for financial support for one year.

Helpful comments and suggestions of the members of the Laboratory staff, including Dr. John O. Rasmussen and Dr. Frank Stephens, Jr., have been greatly appreciated.

The task of alpha-track counting performed by Miss Jacqueline Chang, Mr. James Light, and Mr. Carl Hanke is gratefully acknowledged. Also appreciated is the help from Mrs. Helen Michel during various phases of the work. Sincere thanks are extended to the crews of the 184 inch and the 88-inch cyclotrons for their assistance and cooperation in making the bombardments and to the Health Chemistry staff for their handling of the targets. The assistance of the Chemistry Technical Support Group, in particular of Duane Mosier, is gratefully acknowledged.

Special thanks are accorded to various friends for their constant encouragement.

It is a pleasure to acknowledge the assistance and supervision of Dr. Frank Asaro and the advice of Professor Isadore Perlman, under whose direction the work was undertaken and conducted.

This work was done under the auspices of the U. S. Atomic Energy Commission.



REFERENCES

1. M. Geoppert-Mayer, Phys. Rev. 75, 1969 (1949).
2. O. Haxel, J. H. D. Jensen, and H. E. Suess, Phys. Rev. 75, 1766 (1949).
3. J. L. Blankenship, and C. J. Borkowski, IRE Trans. Nucl. Sci. NS-7, No. 2-3 (1960).
4. J. Chwaszezewska, S. Chaszczewska, and Kazimere-Dybowski, Nukleonika 6, No. 10, 635-641 (1962).
5. Richard C. Pilger, Jr., Nuclear Decay Scheme in the Actinium Family (Ph. D. Thesis), University of California Radiation Laboratory Report UCRL-3877, July 1957 (unpublished).
6. Duane Mosier, Lawrence Radiation Laboratory Report UCRL-10023, p. 224, 1961.
7. A. A. Wydler, A Multiplex Pulse-Height Recorder and Analyzer, Lawrence Radiation Laboratory Report UCRL-9720, May 1961.
8. W. W. Meinke, A. Ghiorso, and G. T. Seaborg, Phys. Rev. 81, 782 (1954).
9. M. W. Hill, Nuclear Decay Studies of Protactinium Isotopes (Ph. D. Thesis), University of California Radiation Laboratory Report UCRL-8423, Aug. 1958.
10. L. A. Sliv and I. M. Band, Coefficients of Internal Conversion of Gamma Radiation (Academy of Sciences, USSR 1956); Translation issued in U. S. A. as University of Illinois Report 57, ICCKI, Physics Department, University of Illinois, Urbana, Illinois, 1956.
11. H. Vartapetian, Compt. Rend. 244, 65 (1957).
12. F. Asaro, F. S. Stephens, J. M. Hollander, and I. Perlman, Phys. Rev. 117, 492-505 (1960).
13. E. L. Church and J. Weneser, Phys. Rev. 104, 1382 (1956).
14. S. G. Nilsson and J. O. Rasmussen, Nucl. Phys. 5, 617-646 (1958).
15. G. Kramer and S. G. Nilsson, Nucl. Phys. 35, 273-94 (1962).
16. A. Bohr and B. R. Mottelson, Kgl. Danske Videnskab. Selskab, Mat.-Fys. Medd. 27, 16 (1953); also Phys. Rev. 89, 316 (1953).

17. I. Perlman and J. O. Rasmussen, in Handbuch der Physik (Springer-Verlag, Berlin, 1957), vol 42, p. 107; Alpha Radio-activity, UCRL-3424, p. 94 (June 1956).
18. S. G. Nilsson, Kgl. Danske Videnskab. Selskab, Mat.-Fys. Medd. 29, No. 16 (1955).
19. A. Bohr, P. O. Froman, and B. R. Mottelson, Kgl. Danske Videnskab. Selskab, Mat.-Fys. Medd. 29, 10 (1955).
20. J. O. Newton, Nucl. Phys. 3, 345 (1957).
21. J. P. Mize and J. W. Starner, Bull. Am. Phys. Soc. Ser. II, 1, 171 (1956).
22. D. Strominger and J. O. Rasmussen, Phys. Rev. 100, 844 (1955).
23. R. W. Hoff, J. L. Olsen, and L. G. Mann, Phys. Rev. 102, 805 (1956).
24. D. Strominger, J. M. Hollander, and G. T. Seaborg, Rev. Mod. Phys. 30, 2, 585 (1958).
25. S. A. Baranov, V. M. Kulakov, P. S. Someilov, A. G. Zelenkev, Yu. F. Radionov, and S. V. Pirozhkov, Zh. Eksperim. i Tear. Fiz. 41, 1475 (1961).
26. F. S. Stephens, F. Asaro, and I. Perlman, Phys. Rev. 113, 211-224 (1959).
- 26a. S. G. Nilsson and O. Prior, Kgl. Danske Videnskab. Selskab, Mat.-Fys. Medd. 32, No. 16 (1961).
27. G. I. Novikov, E. A. Volkova, L. L. Goldin, D. M. Ziv, and E. F. Tret'yakov, Soviet Phys. 10, No. 4 (1960, and J. Expt. Theor. Phys. 37, 928-937 (1959).
28. P. O. Froman, Kgl. Danske Videnskab. Selskab, Mat.-Fys. Skr. 1, No. 3 (1957).
- 28a. V. G. Soloviev, Phys. Letters 1, 202-205 (1962).
29. G. T. Emery, N. F. Fieber, and W. R. Kane, Bull. Am. Phys. Soc. 7, 11 (1962).
30. S. Bjornholm, M. Lederer, F. Asaro, and I. Perlman, Alpha Decay to Vibrational States, Lawrence Radiation Laboratory Report UCRL-9938, Sept. 1962.

31. E. K. Hyde and M. H. Studier, Reported in Argonne Natl. Lab. Report ANL-402, 1948.
32. L. M. Slater and G. T. Seaborg, unpublished data reported in reference 24.
33. Frank Asaro, Lawrence Radiation Laboratory, private communication, 1963.
34. F. S. Stephens, Phys. Rev. 98, 262 A, 1955.
35. F. Asaro and I. Perlman, Lawrence Radiation Laboratory Report UCRL-9524, Jan. 1961.
36. M. Hill, F. Asaro, and I. Perlman, Alpha Decay of Pa<sup>229</sup>, to be published.
37. Helen V. Michel, Hindrance Factors for Alpha Decay, Lawrence Radiation Laboratory Report UCRL-9229, May 1960.
38. S. Rosenblum, E. Cotton, and G. Bouissieres, Compt. Rend. 229, 825 (1949).
39. G. Scharff-Goldhaber and M. MacKeown, Phys. Rev. 82, 123 (1951).
40. T. Meitner, Z. Physik, 50, 15 (1928).
41. J. Teillac, Ann. Phys. 7, 396 (1952).
42. John Philip Hummel, Alpha-Decay Studies in the Heavy-Element Region, (Ph. D. Thesis), University of California Radiation Laboratory Report UCRL-3456, July 1956, (unpublished).
43. F. S. Stephens, Jr., unpublished data reported in reference 24, also private communication.

This report was prepared as an account of Government sponsored work. Neither the United States, nor the Commission, nor any person acting on behalf of the Commission:

- A. Makes any warranty or representation, expressed or implied, with respect to the accuracy, completeness, or usefulness of the information contained in this report, or that the use of any information, apparatus, method, or process disclosed in this report may not infringe privately owned rights; or
- B. Assumes any liabilities with respect to the use of, or for damages resulting from the use of any information, apparatus, method, or process disclosed in this report.

As used in the above, "person acting on behalf of the Commission" includes any employee or contractor of the Commission, or employee of such contractor, to the extent that such employee or contractor of the Commission, or employee of such contractor prepares, disseminates, or provides access to, any information pursuant to his employment or contract with the Commission, or his employment with such contractor.

